Journal of Hydrology 625 (2023) 130121

Contents lists available at ScienceDirect

Journal of Hydrology

journal homepage: www.elsevier.com/locate/jhydrol

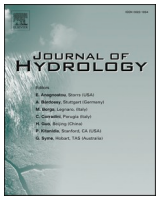

Research papers

Sink or carbon source? how the *Opuntia* cactus agroecosystem interacts in the use of carbon, nutrients and radiation in the Brazilian semi-arid region

Alexandre Maniçoba da Rosa Ferraz Jardim [a,b,*], José Edson Florentino de Morais [c], Luciana Sandra Bastos de Souza [c], Fabio Ricardo Marin [d], Magna Soelma Beserra de Moura [e], Leonor Patricia Cerdeira Morellato [b], Abelardo Antônio de Assunção Montenegro [a], Jean Pierre Henry Balbaud Ometto [f], João L.M.P. de Lima [g], José Carlos Batista Dubeux Júnior [h], Thieres George Freire da Silva [a,c]

[a] *Department of Agricultural Engineering, Federal Rural University of Pernambuco, Recife 52171-900, Pernambuco, Brazil*
[b] *Department of Biodiversity, Institute of Bioscience, São Paulo State University—UNESP, Rio Claro 13506-900, São Paulo, Brazil*
[c] *Academic Unit of Serra Talhada, Federal Rural University of Pernambuco, Serra Talhada 56909-535, Pernambuco, Brazil*
[d] *Department of Biosystems Engineering, University of São Paulo, College of Agriculture "Luiz de Queiroz" – Esalq, São Paulo 13418-900, Brazil*
[e] *Brazilian Agricultural Research Corporation, Embrapa Semiarid, Petrolina 56302-970, Pernambuco, Brazil*
[f] *National Institute for Space Research—INPE, São José dos Campos, SP, 12227-010, Brazil*
[g] *MARE—Marine and Environmental Sciences Centre, ARNET – Aquatic Research Network, Department of Civil Engineering, Faculty of Sciences and Technology, University of Coimbra, Rua Luís Reis Santos, Pólo II - Universidade de Coimbra, Coimbra 3030-788, Portugal*
[h] *North Florida Research and Education Center, University of Florida, 3925 Highway 71, Marianna, FL 32446, USA*

ARTICLE INFO

Keywords:
Eddy covariance
Rainfed cactus
Net ecosystem CO_2 exchange
Evapotranspiration
CAM plant

ABSTRACT

Anthropogenic disturbances directly influence environmental processes and increase the concentration of carbon (C) in the atmosphere. Here, we compare the differences in the seasonality of the balance of carbon, energy, and radiation, as well as seek to identify the interrelationships between these environmental variables and their impact on the growth of *Opuntia* cactus. Data were acquired from an eddy covariance flux tower over a cactus crop agroecosystem (2019–2021) in the Brazilian semi-arid region. In addition, we use plant growth rates, carbon and nutrient stocks, evapotranspiration (ET) and water use efficiency (WUE), and radiation (RUE). We show that the closure of the surface energy balance was 71%, although there are minimal fluxes of available energy lost (29%) by unquantified processes. At all seasons, the highest net ecosystem CO_2 exchange (NEE) rate was between 11:00–13:00 (−5.75 μmol m^{-2} s^{-1}). During the dry and wet-dry season, there was the lowest daily gross primary productivity (GPP) (2.5 μmol m^{-2} s^{-1}) and net radiation—R_n (217.97 W m^{-2}). Ecosystem respiration was more expressive during the wet season (2.41 μmol m^{-2} s^{-1}), and maximum diurnal value of 2.65 μmol m^{-2} s^{-1}. Furthermore, the latent heat flux was higher during the wet season (114.68 W m^{-2}) and lowered in the dry season (9.39 W m^{-2}). The net assimilation rate showed higher values during the dry-wet transition. The dry season presented higher nutrient use efficiency and WUE (14.77 g m^{-2} mm^{-1}). The highest ET occurred during the wet season (227 mm), and RUE was 81.48% higher than in the dry season. Overall, the cactus was a potential C sink during the three years of assessment (NEE: −377 g C m^{-2} $year^{-1}$; GPP: 881 g C m^{-2} $year^{-1}$). The results help us to understand that most of the R_n energy is used in the sensible heat flux (58% ratio).

* Corresponding author.
E-mail addresses: alexandremrfj@gmail.com (A.M.R.F. Jardim), joseedson50@hotmail.com (J.E.F. Morais), sanddrabastos@yahoo.com.br (L.S.B. Souza), fabio.marin@usp.br (F.R. Marin), magna.moura@embrapa.br (M.S.B. Moura), patricia.morellato@unesp.br (L.P.C. Morellato), montenegro.ufrpe@gmail.com (A.A.A. Montenegro), jean.ometto@inpe.br (J.P.H.B. Ometto), plima@dec.uc.pt (J.L.M.P. de Lima), dubeux@ufl.edu (J.C.B. Dubeux Júnior), thieres.silva@ufrpe.br (T.G.F. Silva).

https://doi.org/10.1016/j.jhydrol.2023.130121
Received 6 April 2023; Received in revised form 14 August 2023; Accepted 19 August 2023
Available online 11 September 2023

1. Introduction

Anthropogenic activities are one of the main contributors to the increase in the concentration of carbon (C) in the atmosphere, and this has been causing damage and threats to the survival of various species worldwide. Terrestrial ecosystems, in general, are responsible for exchanging C and energy with the atmosphere, which provides annual sequestration of 3.2 ± 0.6 Pg C, with great spatial and temporal variability between regions of the globe (Del Grosso et al., 2018; Rodda et al., 2021; Yao et al., 2018; Zeng et al., 2020). In agricultural lands, 44% of which are located in arid regions (Kumar et al., 2021), poor soil management, improper cultivation practices, and incorrect species usage can negatively impact the carbon dioxide (CO_2) balance of landscapes (Bilderback et al., 2021; Camelo et al., 2021; Wilson et al., 2002; Zeng et al., 2020).

In pastures composed of grasses and legumes with C3 and C4 photosynthetic metabolism, the ability to sequester C is similar or greater compared to forest ecosystems (Saliendra et al., 2018). Plants that have crassulacean acid metabolism (CAM) photosynthesis, for example, cacti, have reduced water loss and high efficiency in the use of water and carbon (i.e., more efficient than C3 and C4 photosynthesis plants), helping to survive even in places with high-stress conditions, mainly abiotic (de Cortázar and Nobel, 1986; Dubeux Jr. et al., 2006; Jardim et al., 2021a; Nobel and Bobich, 2002; Owen et al., 2016). Cacti of the genus *Opuntia* are extensively cultivated worldwide due to their high adaptability and diverse uses in agricultural, environmental, and industrial systems. The species *Opuntia stricta* (Cactaceae) is specifically utilized in Brazil for its versatility, serving as fodder in water-scarce regions (Jardim et al., 2021b; da Silva et al., 2023), used for both human and animal consumption (Dubeux Jr. et al., 2021; Silva et al., 2023), and also contributing to storing soil organic carbon (Coêlho et al., 2023).

Although cacti have demonstrated promising carbon and water use efficiency (Nobel and Bobich, 2002; Scalisi et al., 2016; Snyman, 2006), to the best of our knowledge, this study represents the first worldwide attempt to quantify carbon-energy fluxes using the eddy covariance technique in the exclusive cultivation of the cactus species *Opuntia stricta*. Notably, in the Sonoran Desert region of the United States, previous studies by Flanagan and Flanagan (2018) and Bilderback et al. (2021) have evaluated CO_2 fluxes in ecosystems composed of *Opuntia* species (e.g., *Opuntia engelmannii* and *Opuntia chlorotica*). These studies have shown C deposition in the soil (Bilderback et al., 2021) and have indicated that the photosynthetic activity of cacti exceeds respiration (Flanagan and Flanagan, 2018). However, flux information specific to *Opuntia stricta* is still limited.

For many decades, monitoring of environmental conditions has been carried out by flux towers in various biomes and surfaces (Baldocchi et al., 2000; Costa et al., 2022; Cunliffe et al., 2022; McGloin et al., 2018). Among the applied techniques, the eddy covariance method is well established in several parts of the world, measuring latent heat (*LE*) fluxes and the net ecosystem CO_2 exchange (NEE) (Cunliffe et al., 2022; Flores-Rentería et al., 2023). In this method, the *LE* and NEE results are measured by the transport of turbulent fluxes in the boundary layer of the vegetation canopy and atmosphere (Anapalli et al., 2019). In turn, the high-frequency data—generally measured at 10 to 20 Hz by the eddy covariance system such as the *LE*, can be used to determine the evapotranspiration (ET) of the crop, and the NEE carbon flux can be partitioned in gross primary production (GPP) and ecosystem respiration (R_{eco}), aiding in the understanding of crop water and the local carbon budget (Anapalli et al., 2019; Cunliffe et al., 2022; Flores-Rentería et al., 2023; Guevara-Escobar et al., 2021).

In places with average annual precipitation of 200–700 mm, as is the case in a semi-arid environment (Kumar et al., 2021), understanding the C balance, and the specific responses of the net ecosystem exchange of CO_2, gross primary production and ecosystem respiration at different times of the year help to understand how vegetation behaves as a carbon sink and source. According to Mendes et al. (2020), evaluating the Caatinga biome, a typical dry ecosystem with the presence of cacti, grasses, and tree-shrub species, found NEE results ranging from –169.0 to –145.0 g C m^{-2} $year^{-1}$, with a strong influence of the GPP in the wet and dry seasons. Flores-Rentería et al. (2023) evaluated xerophilous shrubland in the Chihuahuan Desert of Northeast Mexico, with species of *Opuntia* spp. and other CAM plants (e.g., *Agave asperrima*, *Cylindropuntia leptocaulis*) found annual NEE of –303.5 g C m^{-2}, GPP of 841.3 g C m^{-2}, and cumulative R_{eco} of 537.7 g C m^{-2}. These authors concluded that the ecosystem was a sink during most of the year because the vegetation is adapted to grow and absorb C under arid conditions. Notably, information on cactus ecosystems is lacking, with some of these processes of carbon fluxes and stocks being difficult to quantify.

Thus, the hypothesis that motivated this research was—do cactus crops have a high CO_2 absorption capacity for long periods, and can they be efficient even in dry seasons? Based on the rationale for this hypothesis, the objectives of this study were (1) to compare the differences in the seasonality of the balance of carbon, energy, and radiation and (2) to identify the interrelationships between fluxes of carbon, energy and radiation, meteorological variables and its impacts on the growth of cactus plants (*Opuntia stricta*) cultivated in a semi-arid environment. The findings and details of the dynamics of CO_2 and energy fluxes during the seasons can inform agricultural management decisions and provide a baseline for future work aimed at carbon sequestration in cactus agroecosystems.

2. Materials and methods

2.1. Study site description

The study was conducted in a crop field located in the municipality of Floresta, State of Pernambuco, Brazil (8°18′ S, 38°30′ W, and 367 m above mean sea level) (Fig. 1a). The climate is characterized by irregular rainfall from December to April, classified as hot semi-arid (BSh). The annual average rainfall, relative humidity (*RH*), and air temperature are 489 mm, 61% and 26.1 °C, respectively, and 2023 mm $year^{-1}$ of reference evapotranspiration. The dominant wind direction is Southeast, with an average annual speed of 1.8 m s^{-1}. The soil has a sandy loam texture (56% sand, 41% silt, and 3% clay) of the Chromic Luvisols type, with a bulk density of 1.33 g cm^{-3}, total porosity of 48.05%, pH of 5.35, the electrical conductivity of 0.28 dS m^{-1}, cation exchange capacity of 8.08 $cmol_c$ dm^{-3} and base saturation of 78.60%. All soil samples were collected from the 0–0.40 m depth layer. Soil pH and electrical conductivity were determined in a 1:2.5 soil/distilled water suspension. The average slope at the site is less than 1%.

Data were collected between January 2019 and December 2021 at a site cultivated with cactus [*Opuntia stricta* (Haw.) Haw.] (henceforth called *Opuntia*), species resistant to *Dactylopius opuntiae* Cockerell (Hemiptera: Dactylopiidae). In August 2014, cactus planting and conventional soil preparation were carried out, i.e., plowing, harrowing, and furrowing. We used single crop rows spaced 2.0 × 0.5 m, totaling a plant density of 10,000 plants ha^{-1} (Fig. 1b–c). After soil preparation, the cladodes were planted, keeping the lower base inserted at 50% of the soil surface. Minimal cultural practices (hand weeding) were carried out for weed management since there was no herbicide registered for *Opuntia*, and this caused the emergence of *Sida* spp. during the trial period. In addition, the cactus plants were grown in rainfed conditions throughout the experimental period, and no fertilization was applied.

Based on the climatic conditions, we differentiated the wet and dry seasons from 2019 to 2021 into four seasons: wet, dry, transitional dry-wet and wet-dry (see Supplementary Material Table S1). For example, the wet season is when the accumulated rainfall in five or more consecutive days is at least 20 mm, without any dry period exceeding seven days during the following 30 days. If in 30 days the accumulated rainfall is less than 20 mm with less than five days of rainfall, the dry season occurs. On the other hand, if none of these criteria are met, the

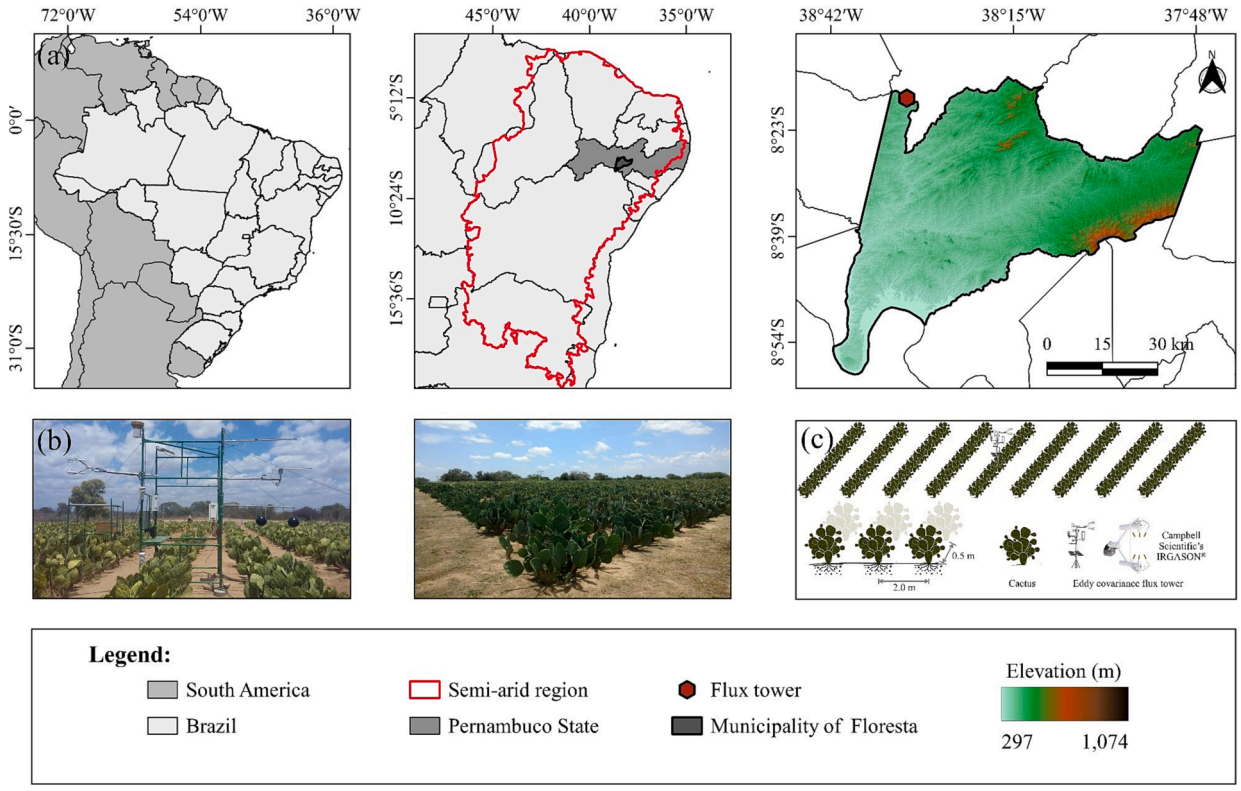

Fig. 1. Description and geographical location of the study area (a). Flux tower with eddy covariance system, cultivation of *Opuntia stricta* cactus (b), and schematic layout of the experimental field (c).

dry-wet or wet-dry transition season occurs, the first being after the dry season and the second after the occurrence of the wet season. This delimitation was to explore the role of seasonal hydrological components as a function of the onset and end of rainfall (Leite-Filho et al., 2019; Salack et al., 2016).

2.2. Measurements of environmental variables

Micrometeorological measurements were performed using a 3 m high tower installed above the cactus canopy near the center of the experimental area. To measure the net radiation (R_n) components, we used closed-cell thermopile-style sensors (NR-Lite, Kipp & Zonen, Delft, Netherlands) in addition to net radiometers (SP-230, Apogee Instruments, Logan, Utah, USA) that measure upward and downward shortwave and longwave radiation. Each radiometer sensor was installed 2.8 m above the canopy to quantify the incident radiation and another one for the radiation reflected by the canopy, i.e., sensors positioned up- and down-looking. Photosynthetically active radiation (PAR) was measured with a quantum sensor (LI-190SB, LI-COR, Inc., Lincoln, Nebraska, USA) mounted at the top and bottom of the canopy. Soil heat flux (G) was measured using a heat flux plate (HFT3, REBS, Hukseflux, Delft, Netherlands) installed at a depth of 0.05 m close to the cactus crop line. Air temperature and *RH* were measured by two thermo-hygrometers (HMP45C, Campbell Scientific, Logan, Utah, USA), creating a vertical profile 0.5 and 1.5 m above the soil surface. Rainfall was measured using an automatic rain gauge (CS700-L, Hydrological Services Rain Gauge, Liverpool, Australia) positioned 3 m above the soil surface to avoid interference from tower structures. Soil moisture (m^3 m^{-3}) was quantified at a depth of 0.30 m using a time domain reflectometry (TDR) probe (CS616, Campbell Scientific, Logan, UT, USA) buried vertically in the soil next to the eddy covariance tower. Data from the micrometeorological sensors were recorded by a CR3000 data logger (Campbell Scientific Inc., Logan, Utah, USA) every 60 s, with a storage interval of 10 min. Measurements were collected continuously during the daytime and nighttime.

2.3. Flux measurements and data processing

Flux measurements with the eddy covariance system were performed using an open-path CO_2/H_2O gas analyzer and a sonic anemometer (IRGASON; Campbell Scientific Inc., Logan, Utah, USA), with data stored in averages of 30 min on a CR3000 data logger (Campbell Scientific Inc., Logan, Utah, USA). The IRGASON is a system that combines an open-path infrared gas analyzer (IRGA) together with a three-dimensional sonic anemometer (Fig. 1b–c). The sensor was fixed during the entire experimental period at 2.0 m above ground level, oriented towards the Southeast (135°) in favor of the predominance of the wind, to ensure that the measurements were contained in the appropriate coverage area of the flux system. In this way, the average value of the fetch/height ratio in almost stable conditions was 65:1. For calculations of latent heat flux (LE), sensible heat flux (H), and CO_2 flux, we used EasyFlux PC software (Campbell Scientific Inc.) which performs high frequency (10 Hz) raw data corrections, generating averages every 30 min. During the post-processing step in EasyFlux all necessary corrections were applied, including outlier removal (Vickers and Mahrt, 1974), bias correction (Rannik and Vesala, 1999), rotation of two-dimensional coordinates (Wilczak et al., 2001), sonic temperature correction (Schotanus et al., 1983), and frequency response (Moore, 1986) and Webb-Pearman-Leuning density corrections (Webb et al., 1980). In addition, flux measurements were classified according to three quality criteria: high, moderate, or low-quality data (Yang et al., 2022). In this step, only high- and moderate-quality flux measurements were used. Finally, after the post-processing step and quality filtering, 94% of the CO_2 flux data were suitable for analysis.

We used the online platform developed by the Max Planck Institute for Biogeochemistry in Jena, Germany (https://www.bgc-jena.mpg.de/~MDIwork/eddyproc/) to perform the partitioning of the net ecosystem CO_2 exchange (NEE) (Wutzler et al., 2018). NEE was monitored using

the eddy covariance technique and refers to the net exchange of CO_2 between the ecosystem and the atmosphere, basically composed of gross primary productivity (GPP) and ecosystem respiration (R_{eco}), the latter being equivalent to the sum of autotrophic and heterotrophic respiration. In the present study, we used the meteorological convention, i.e., negative NEE values indicate CO_2 absorption in the ecosystem, while positive values indicate net CO_2 loss to the atmosphere. With the adjusted *LE* data measured by the eddy covariance system, we converted it to evapotranspiration—ET in millimeters (mm) through the latent heat of water vaporization (2.45 MJ kg^{-1}) (Salazar-Martínez et al., 2022).

2.4. Surface energy budget

The estimate of Earth's surface radiation was made through the energy balance between short and longwave radiation described as follows:

$$SR_n = SR_d - SR_u \quad (1)$$

$$LR_n = LR_d - LR_u \quad (2)$$

$$R_n = SR_n + LR_n \quad (3)$$

where SR_n is the net shortwave radiation, SR_d is the downward shortwave radiation, SR_u is the upward shortwave radiation (i.e., reflected outgoing shortwave radiation), LR_n is the net longwave radiation, LR_d is the downward longwave radiation, LR_u is the upward longwave radiation, and R_n is the net radiation. All radiation variables were measured in W m^{-2}. Still using ascending and descending shortwave radiation, we calculated the albedo (α) of the cultivated surface with cactus:

$$\alpha = \frac{SR_u}{SR_d} \quad (4)$$

2.5. Energy budget partitioning

In this paper, we use the simplified version of the surface energy balance method (Eq. (5)). This method is based on the principle of conservation of energy:

$$R_n = LE + H + G \quad (5)$$

where *LE* is the latent heat flux (W m^{-2}), *H* is the sensible heat flux (W m^{-2}), and *G* is the soil heat flux (W m^{-2}).

All data sets are presented in local time (i.e., 3 h behind Greenwich Mean Time). Furthermore, energy from metabolic activities, heat storage in plant tissue and canopy, and horizontal advection were omitted and considered insignificant (Papale et al., 2006). Thus, these energy components were not included in our energy balance algorithm. The components described in Eq. (5) are normally positive during the daytime, with net radiation and soil heat flux positive downwards and latent and sensible heat fluxes positive upwards.

2.5.1. Energy balance closure

A common feature when using measurements with eddy covariance is the lack of closure of the surface energy budget. Thus, the sum of latent and sensible heat fluxes ($LE + H$) is commonly smaller than the measured available energy ($R_n - G$), which causes an energy imbalance in the system (Dhungel et al., 2021; Widmoser and Wohlfahrt, 2018). To analyze the energy balance closure (EBC), we fitted an origin-forced linear regression model to the half-hour data, establishing a relationship between the turbulent fluxes as the dependent variable and the available energy as the independent variable (McGloin et al., 2018). This type of linear regression approach provides a stable and robust estimate of energy balance closure, even when available energy is close to zero. Furthermore, we do not use any technique for forcing the closure of the energy balance. Here, the quotient of latent and sensible heat fluxes and available energy expresses the EBC:

$$EBC = \frac{(LE + H)}{(R_n - G)} \quad (6)$$

2.6. Biomass yield and growth allometry

We determined the biomass yield produced each year and season by weighing four randomly selected representative plants, which exhibited a consistent pattern of growth and development. The aboveground plant biomass was harvested entirely and weighed on an electronic balance to quantify the fresh matter (g FM $plant^{-1}$) and subsequently dried in a forced air circulation oven at 55 °C until reaching a constant weight. Here, we determined the weight of dry matter per plant (g DM $plant^{-1}$); thus, the productivity of cacti was estimated in grams per square meter per season or year (g m^{-2} $season^{-1}$ and g m^{-2} $year^{-1}$, respectively). In addition, morphometric data and plant biomass were collected monthly, with five plants being measured to compose the morphometric data and another four plants collected for biomass analysis over time. For each plant, we quantified the cladode and plant morphometric variables. In cladode structures, the length and width were measured, as well as the number of cladodes (units), by counting cladodes in order of appearance in the plant (i.e., first order, second order, third order and so on) and the total number of cladodes, i.e., through the sum of cladodes by order. For plant height measurements, we considered the vertical distance from the ground to the canopy apex, and the plant width was across two widths from the canopy edge. Then, the collected samples were used to quantify the morphophysiological indices of the cacti.

In our study, Equations (7) and (8) were used to determine the cladode area—CA and the cladode area index—CAI (Pinheiro et al., 2014; Silva et al., 2014). Furthermore, with data on dry mass yield and cladode parameters, we calculated the morphophysiological indices of *Opuntia* using a sigmoidal model with three parameters (Eq. (9)) (Jardim et al., 2023).

$$CA = 0.7086 \times \left[\frac{1 - e^{(-0.000045765 \times CL \times CW)}}{0.000045765}\right] \quad (7)$$

$$CAI = \left[\sum_{n}^{i=1} (CA) / \frac{10,000}{(S1 \times S2)}\right] \quad (8)$$

$$y = \frac{a}{1 + e^{\left(\frac{-x-x0}{b}\right)}} \quad (9)$$

where CL is the cladode length (cm), CW is the cladode width (cm), *i* is the observation number, *n* is the total number of observations, 10,000 is the conversion factor from cm^2 to m^2, and S1 × S2 is the spacing between the rows and plants of each cactus (i.e., 2.0 × 0.5 m), respectively. Here, the parameters for the morphophysiological analysis were: y is the response variable (e.g., cladodes dry matter, cladode area index, and the number of cladodes), a is the maximum value for the rate (i.e., the distance between the two asymptotes), x is the accumulated days, x0 is the number of days necessary for the plant to express 50% of the maximum rate (i.e., the inflection point of the curve), and b is the number of days necessary for the start of the rate.

Next, we quantified the relative growth rate—RGR (g g^{-1} day^{-1}), net assimilation rate—NAR (g m^{-2} day^{-1}), and specific cladode area—SCA (m^2 g^{-1}) (Jardim et al., 2023; Khapte et al., 2022). The RGR is determined by fitting the increase in dry biomass with the accumulated biomass over time. NAR represents the dry mass produced by cladode area per unit of time, and this variable is commonly used to represent the net photosynthesis rate of plants. The SCA refers to the cladode area useful for photosynthesis (Jardim et al., 2023). All growth rates were calculated during the experimental period of the plants, from 2015 to 2021.

2.7. Resource use efficiencies

2.7.1. Water use efficiency

The water use efficiency (WUE, g m^{-2} mm^{-1}) was calculated by dividing the crop biomass yield and its evapotranspiration (Zhang et al., 2022b):

$$WUE = \frac{DMY}{ET} \quad (10)$$

where DMY is the dry matter yield (g m^{-2}), and ET is the evapotranspiration (mm).

2.7.2. Radiation use efficiency and interception photosynthetically active radiation

The radiation use efficiency (RUE, g MJ^{-1}) over the entire experimental period was calculated using the following equation (Raza et al., 2019):

$$RUE = \frac{DMY}{I_0 \times fIPAR} \quad (11)$$

where I_0 is the amount of daily-incident photosynthetically active radiation (PAR) above the canopy (MJ m^{-2}), and *f*IPAR is the fraction of PAR intercepted (400–700 nm). Therefore, we can calculate *f*IPAR using lows:

$$fIPAR = \left(1 - \frac{PAR_b}{I_0}\right) \quad (12)$$

$$fIPAR = 1e(-k \times CAI) \quad (13)$$

where PAR_b is the PAR measured below the plant canopy, and *k* is the light extinction coefficient based on the Beer-Lambert law.

2.7.3. Nutrient stocks and use efficiency

Above-ground dry biomass was ground to powder using a Wiley-type mill (Model 4, Thomas-Wiley Laboratory Mill, Thomas Scientific, Swedesboro, NJ, USA) with a 1 mm sieve. The nutrients presented here were chosen because they are essential and indispensable for the growth and development of cactus plants. Then, we carried out an analysis of the concentration of mineral elements in the plant tissue of the plants. The micro-Kjeldahl method determined the cladode's total nitrogen content (N, mg kg^{-1}) (Santos et al., 2020). Phosphorus (P, mg kg^{-1}) was measured by the vanado-molybdate method with UV–visible spectrophotometry reading at 430 nm (Du Toit et al., 2018). Meanwhile, the potassium (K^+, mg kg^{-1}) was determined by a flame photometer (Rodrigues et al., 2013). To determine calcium (Ca^{2+}, mg kg^{-1}) and magnesium (Mg^{2+}, mg kg^{-1}), we used an atomic absorption spectrophotometer (Loupassaki et al., 2007). The dry biomass's carbon content (C, mg kg^{-1}) was determined by the Dumas method via dry combustion (Adamič and Leskovšek, 2021). Finally, the nutrient use efficiency (NUE, mg m^{-2} mm^{-1}) was calculated according to Eq. (14). The nutrient stock (g m^{-2}) was obtained by multiplying the dry biomass per square meter by the nutrient concentration.

$$NUE = \frac{DMY \times Nu}{ET} \quad (14)$$

where *Nu* is the concentration of the nutrient in the analyzed sample of plant tissue. Eq. (14) was adapted (Zhang et al., 2020), making it a function of crop evapotranspiration. This adaptation provides more clarity in understanding the nutrient uptake capacity of the plant from the soil solution, together with the consumption of water lost through evapotranspiration.

2.7.4. Carbon stock and efficiency

Using the carbon that was quantified in the plants' dry biomass (without the root biomass), we quantified the carbon use efficiency—CUE (μg m^{-2} mm^{-1}). Thus, based on Eq. (14), the efficiency in the use of carbon was realized. Furthermore, the carbon stock (g m^{-2}) was calculated by multiplying the elemental carbon concentration by the dry biomass produced per square meter (Siddiq et al., 2021).

2.8. Statistical analysis

In this study, we use the linear regression method to quantify the energy balance closure of the eddy covariance system through the ratio between available energy and turbulent heat fluxes during the experimental period. We fitted non-linear regression models (sigmoidal model) for plant growth rates. The components of carbon, energy, and radiation balances during the four seasons were presented in curves and boxplots over time (i.e., hour, month, year and station). All boxplots include median, whiskers, and 1.5 times the upper and lower interquartile ranges. Subsequently, we applied principal component analysis (PCA) to examine the interrelationships between seasons and environmental and cactus plant parameters. PCA is a type of multivariate analysis that reduces large data sets through orthogonal transformation, generating linearly uncorrelated variables called principal components (Lamichhane et al., 2021). In this way, the new set of data generated by the PCA provides new values, called scores and loadings, and are visualized in biplots in multivariate space. Furthermore, before performing the PCA, all variables were standardized using the z-transformation, with zero mean and unit standard deviation. Finally, the significant principal components (PCs) were selected according to the Kaiser criterion, considering only eigenvalues greater than 1.0 (Jardim et al., 2021a; Kaiser, 1960; Lamichhane et al., 2021). All data processing and analysis were performed using the R program version 4.1.3 (R Core Team, 2022).

3. Results

3.1. Energy balance closing overview and environmental conditions during the experimental period

Our result of the EBC during the study period (2019 to 2021) was 0.71, and the coefficient of determination of 0.94 ($P < 0.001$) (Fig. S1 in the Supplementary Material). The horizontal and vertical coordinate boxplots show that the fluxes are concentrated at 316.83 and 236.69 W m^{-2}, respectively, and the rest of the scattered data above the mean are causing a slope of the line for available energy. Although there is a high EBC value, minimal fluxes of available energy are being lost (29%) by unquantified processes, e.g., heat storage in the canopy.

During the study period, the average air temperature was 26.58 °C, with minimum (July 2020) and maximum (November 2019) values of 23.25 and 29.77 °C, respectively (see details in Supplementary Material, Fig. S2a). The relative humidity average was 49.57%, with the wettest months from February to May being 16.78% higher than the annual average (Fig. S2b). The VPD showed an average of 1.94 kPa, with the most deficit period from April to July, and 2021 with the lowest average (1.88 kPa). The mean annual rainfall was 820.32 mm, 67.76% above the climatological normal for the municipality (489 mm $year^{-1}$). In addition, the soil moisture ranged from 0.08 to 0.29 m^3 m^{-3}, and the months from February to May showed the highest results (Fig. S2f). We observed values of 19.31 and 7.91 MJ m^{-2} day^{-1} for R_g and PAR, respectively (Fig. S2g–h).

3.2. Seasonal and temporal variation in the balance of carbon, energy and radiation

Fig. 2 shows half-hourly averages of carbon (C), energy, and radiation exchanges in *Opuntia* cactus cultivation across four seasons: dry, dry-wet transition, wet, and wet-dry transition (see Table S1). Nighttime NEE indicated CO_2 release, while dawn showed increased CO_2 absorption (Fig. 2a). The highest daytime absorption rate, averaging −5.75 μmol m^{-2} s^{-1}, occurred between 11:00 and 13:00. Wet, wet-dry and dry-

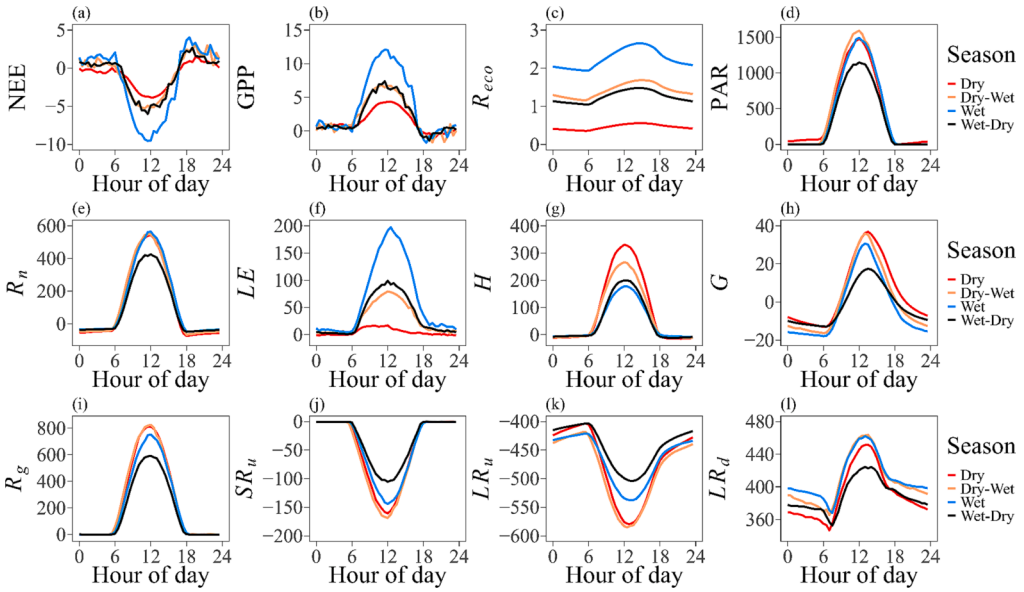

Fig. 2. Diurnal cycle of carbon exchange, energy budget, and hourly radiation during dry and wet seasons (i.e., dry season, dry-wet transition, wet season, and wet-dry transition) in cactus cultivation in the Brazilian semi-arid region. (a) Net ecosystem CO_2 exchange—NEE, (b) gross primary productivity—GPP, (c) ecosystem respiration—R_{eco}, (d) photosynthetic active radiation—PAR, are expressed in μmol m^{-2} s^{-1}. (e) Net radiation—R_n, (f) latent heat flux—LE, (g) sensible heat flux—H, (h) soil heat flux—G, (i) global solar radiation—R_g, (j) upward shortwave radiation—SR_u, (k) upward longwave radiation—LR_u, and (l) downward longwave radiation—LR_d, all expressed in W m^{-2}. Negative values in panel (a) indicate carbon uptake while positive values in panels (b) and (c) indicate carbon release by the ecosystem.

wet transition seasons displayed similar and more negative average absorption rates of −6.42 μmol m^{-2} s^{-1}, 71.23% higher than the dry season. Wet season GPP averaged 7.03 μmol m^{-2} s^{-1} (range: −1.27 to 12.06 μmol m^{-2} s^{-1}) (Fig. 2b). The dry season had lower diurnal GPP (2.5 μmol m^{-2} s^{-1}). R_{eco} was higher during the wet season (2.41 μmol m^{-2} s^{-1}, maximum: 2.65 μmol m^{-2} s^{-1}). The dry-wet, wet-dry, and dry seasons exhibited R_{eco} values 37.03%, 44.21%, and 79.49% lower than the wet season, respectively (Fig. 2c). We observed higher PAR during the dry-wet transition season (average: 915.05 μmol m^{-2} s^{-1}), while the dry and wet seasons showed no significant difference (average: 838.17 μmol m^{-2} s^{-1}). The wet-dry transition season had the lowest PAR value recorded (656.38 μmol m^{-2} s^{-1}) (Fig. 2d).

In the study, R_n values during the wet-dry transition were smaller (217.97 W m^{-2}) with a peak at noon (Fig. 2e). However, no significant difference was observed between the dry season, dry-wet transition, and wet season, with an average value of 283.11 W m^{-2}. The wet season exhibited higher values of LE (114.68 W m^{-2}) compared to the dry season (9.39 W m^{-2}). The wet-dry season had a slightly lower average LE of 60.05 W m^{-2}, down by 17.57% compared to the dry-wet transition (Fig. 2f). The H reached its peak during the dry season (183.33 W m^{-2}) and was lowest in the wet season (93.82 W m^{-2}). Both the dry-wet (19.07%) and wet-dry (43.08%) transitions showed decreased H compared to the dry season. Notably, G followed the pattern of the dry season > dry-wet transition > wet season > wet-dry transition, peaking between 13:00 and 14:00, ranging from 36.90 to 17.42 W m^{-2} between the dry season and the wet-dry transition season, respectively.

In general, the radiation balance was lowest during the wet-dry transition season. For example, R_g in the wet-dry transition was on average 21.02% lower than the wet season, 27.98% lower than the dry season, and 29.88% lower than the dry-wet transition (Fig. 2i). We also observed the same tendency for shortwave—SR_u and longwave—LR_u radiation (Fig. 2j–k). Our results show no difference between the wet season and the dry-wet transition (average: 422.99 W m^{-2}) for LR_d. As for the dry season, the average was 408.93 W m^{-2}, followed by the wet-dry transition (398.03 W m^{-2}).

Fig. 3 shows the cactus agroecosystem response to carbon, energy

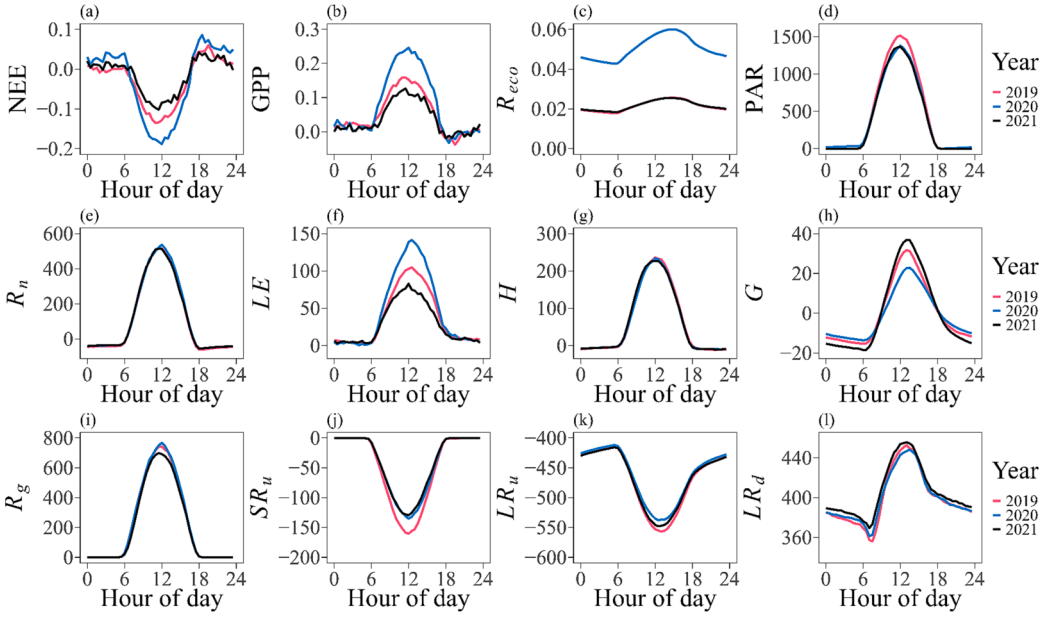

Fig. 3. Variation of carbon exchange, energy budget and radiation on an hourly scale during 2019–2021 in cactus cultivation in the Brazilian semi-arid region. (a) Net ecosystem CO_2 exchange—NEE, (b) gross primary productivity—GPP, (c) ecosystem respiration—R_{eco}, are expressed in g C m^{-2}, and (d) photosynthetic active radiation—PAR, is expressed in μmol m^{-2} s^{-1}. (e) Net radiation—R_n, (f) latent heat flux—LE, (g) sensible heat flux—H, (h) soil heat flux—G, (i) global solar radiation—R_g, (j) upward shortwave radiation—SR_u, (k) upward longwave radiation—LR_u, and (l) downward longwave radiation—LR_d, all expressed in W m^{-2}. Negative values in panel (a) indicate carbon uptake while positive values in panels (b) and (c) indicate carbon release by the ecosystem.

and radiation exchanges on an annual scale (2019–2021). In 2021, there was an apparent decrease in NEE on a diurnal scale, while 2019 and 2020 were more expressive sinks (Fig. 3a). The GPP showed a concave parabolic curve, with a peak occurring at noon and daytime averages of 0.07 g C m^{-2} in 2021, 0.09 g C m^{-2} in 2019, and 0.15 g C m^{-2} in 2020 (Fig. 3b). Here, we reveal that the cactus agroecosystem becomes a C sink as R_g increases. During 2020, which was particularly wet, R_{eco} was higher than in 2021 and 2019, and the highest values occurred between 13:30 and 16:30 (Fig. 3c). Overall, the R_{eco} rate in 2020 was approximately 135% higher than in 2021 and 2019. The C budget was also boosted by the increase in PAR, although there were no differences between 2020 and 2021 (Fig. 3d).

Despite high values of R_n and H, averaging a peak of 522.36 and 232.10 W m^{-2}, respectively, no significant changes were observed between 2019 and 2021 (Fig. 3e, g). However, LE showed year-to-year variations after 7:30, reaching a maximum around noon. In 2020, LE averaged 82.78 W m^{-2}, while in 2021 and 2019, it showed lower diurnal responses, averaging 49.57 and 63.52 W m^{-2}, respectively (Fig. 3f). We found a large variation in G, with 2021 recording the highest value of 12.79 W m^{-2}. The sharpest decline in G occurred after 14:00 across all years (Fig. 3h). Additionally, there were slight differences in the peaks of R_g during 2019–2021, with greater losses (more negative values) of short and long radiation by the cactus surface (Fig. 3i–k). LR_d was slightly higher in 2021, averaging 419.96 W m^{-2} (range: 369.49 to 455.70 W m^{-2}) (Fig. 3l).

Fig. 4 shows the monthly variability of carbon balance and PAR absorbed (APAR) by *Opuntia* cactus from 2019 to 2021. The cactus predominantly acted as a C sink each month (Fig. 4a). The most negative monthly mean NEE values in 2019 occurred in January and April (−2.75 and −3.27 g C m^{-2} day^{-1}, respectively). In 2020, high NEE values were observed in February (−2.78 g C m^{-2} day^{-1}) and March (−3.25 g C m^{-2} day^{-1}), while in 2021, September and October, averaging −1.20 g C m^{-2} day^{-1} and −1.21 g C m^{-2} day^{-1}, respectively. The GPP ranged from 0.59 to 7.21 g C m^{-2} day^{-1}, with an average of 2.61 g C m^{-2} day^{-1} over the entire period (Fig. 4b). R_{eco} showed similar variations across the years, with higher respiration rates observed between March and May and more pronounced peaks in 2020 (Fig. 4c). In 2019, lower R_{eco} values (average: 1.03 g C m^{-2} day^{-1}) coincided with higher NEE and APAR by the cactus. APAR exhibited substantial variations, ranging from a minimum of 2.46 MJ m^{-2} day^{-1} in November 2020 to a maximum of 5.55 MJ m^{-2} day^{-1} in April 2019 (Fig. 4d).

There were significant variations in the energy balance between months and years in cactus cultivation (Fig. 5). The lowest mean value of R_n was found in May–July (9.61 MJ m^{-2} day^{-1}); by contrast, fluxes were higher at the beginning and end of the year (Fig. 5a). In 2019, the months with the lowest LE were September–November; in 2020, they were August–October, followed by 2021 with the lowest LE responses in June–October. High values of H were associated with a reduced contribution to LE (Fig. 5b–c). Notably, the variation pattern of G closely resembled that of H (Fig. 5d). Peaks in G were observed at the beginning and end of the year, with the highest flux occurring in October 2019 (0.51 MJ m^{-2} day^{-1}). In contrast, the lowest G was recorded in February 2020 (−0.40 MJ m^{-2} day^{-1}), attributed to rainfall events (see Fig. S2e).

On average, the R_g varied between 13.86 and 24.31 MJ m^{-2} day^{-1}, with the minimum and maximum values occurring in May 2021 and October 2020, respectively (Fig. 6a). At the beginning of the year, SR_u is higher (more negative), and at the end, it is more pronounced (Fig. 6b). Our LR_u results were similar to SR_u, but with different magnitudes, with longwave radiation lost more significantly (Fig. 6c). After January and February of each year, there was a gradual decrease in LR_u until mid-year, ranging from −36.87 to −43.15 MJ m^{-2} day^{-1}. Meanwhile, LR_d showed significant variations (32.16 to 36.49 MJ m^{-2} day^{-1}) (Fig. 6d).

3.3. Characteristics of seasonal changes in radiation, energy, carbon and water fluxes

The wet-dry transition season showed the lowest values of radiation balance components and had a 26.74% lower R_g compared to other stations (Table S2 in the Supplementary Material). Additionally, this season showed the lowest results of short and long radiation and R_n for the cactus surface. In the dry season, LE was lower than in all seasons, resulting in a significant increase in H (7.9 MJ m^{-2} day^{-1}), followed by 6.4 MJ m^{-2} day^{-1} during the dry-wet transition season. During the wet seasons, G had more negative values, indicating greater energy loss, while in the dry seasons, G showed positive values, indicating higher energy for soil heating. Our findings indicate that the cactus acted as a carbon sink in all seasons and years, with more prominent values during the dry (−1.0 g C m^{-2} day^{-1}) and wet (−1.6 g C m^{-2} day^{-1}) seasons. Furthermore, the NEE during the wet-dry transition season was 55.06% lower than in the wet season (Table S2).

During the dry season, GPP showed the lowest results (1.5 g C m^{-2} day^{-1}). We found that the dry season had a lower carbon efflux due to low R_{eco}, resulting in a high NEE response (Table S2). In contrast, the wet season, influenced by higher rainfall (average of 733 mm), showed a 318.73% higher R_{eco} compared to the dry season. The radiation and energy balances were similar on an annual and crop cycle scale. The first

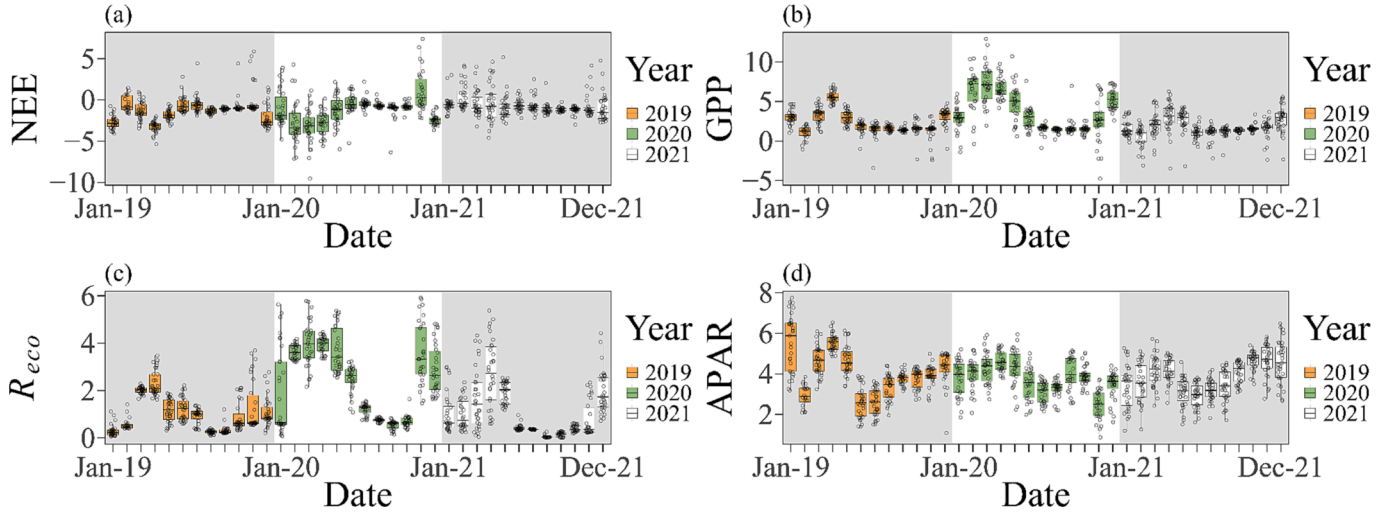

Fig. 4. Monthly variation of carbon balance (i.e., net ecosystem CO_2 exchange—NEE, gross primary productivity—GPP, and ecosystem respiration—R_{eco}) and absorbed photosynthetically active radiation (APAR) in *Opuntia* cactus cultivation during 2019–2021 in the Brazilian semi-arid region. The shaded areas indicate the boundaries of the years. Note: NEE, GPP, R_{eco} in g C m^{-2} day^{-1}, and APAR in MJ m^{-2} day^{-1}.

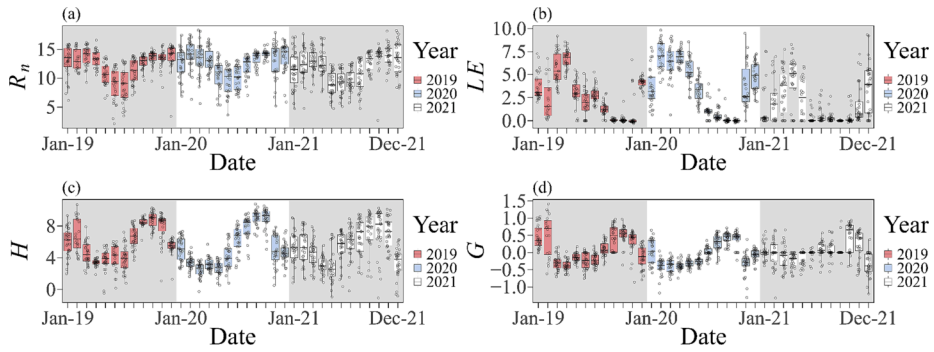

Fig. 5. Diurnal variation of (a) net radiation—R_n, (b) latent heat flux—*LE*, (c) sensible heat flux—*H*, and (d) soil heat flux—*G* during the period 2019–2021 in *Opuntia* cactus cultivation in the Brazilian semi-arid region. All the variables were measured in MJ m^{-2} day^{-1}. The shaded areas indicate the boundaries of the years.

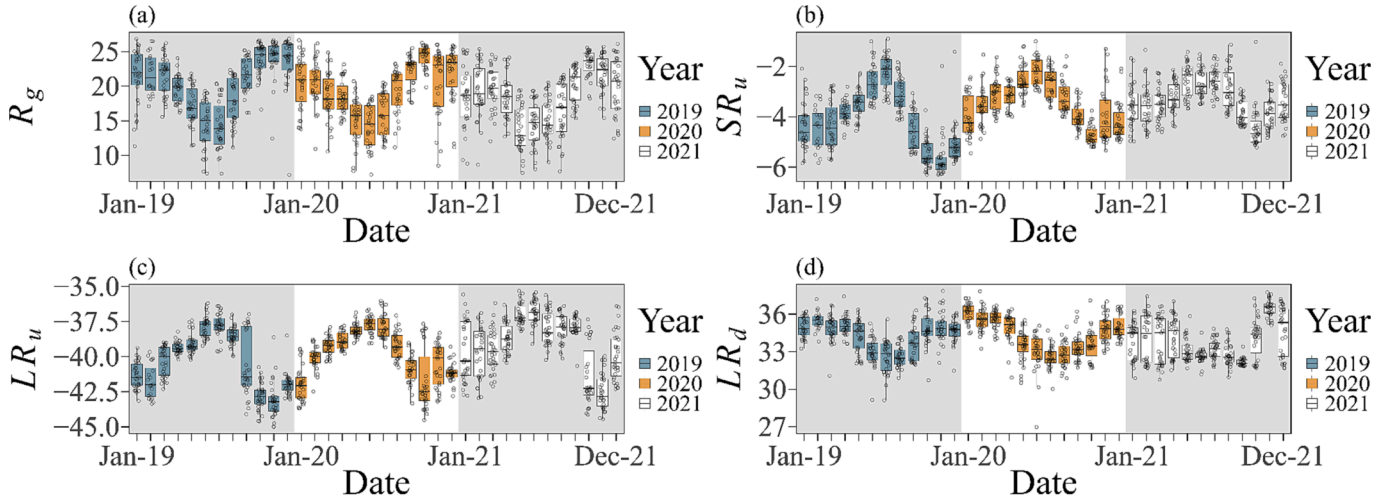

Fig. 6. Temporal variation of radiation balance in *Opuntia* cactus cultivation in the Brazilian semi-arid region. (a) R_g is the global solar radiation, (b) SR_u is the upward shortwave radiation, (c) LR_u is the upward longwave radiation, and (d) LR_d is the downward longwave radiation. All the variables were measured in MJ m^{-2} day^{-1}. The shaded areas indicate the boundaries of the years.

cactus cycle had greater carbon accumulation and higher productivity, with a total C efflux difference of 39.6% compared to the second cycle. It is observed that the rainfall increased the ET, R_{eco}, and GPP in a contrasting way. Furthermore, during the wet season, ET may have been higher due to greater soil evaporation. Notably, ET was more significant in the first cactus cycle, accumulating 819 mm, but decreased by more than half in the second cycle.

3.4. Flux partitioning

Our results of partitioning the radiation and energy fluxes, as well as the *f*IPAR in the cactus agroecosystem, are shown in Supplementary Material Table S3. The SR_u/R_g ratio ranged from 0.16 to 0.22 across seasons and years. R_n accounted for 64% and 60% of global radiation during the wet season and wet-dry transition, respectively. The PAR/R_g ratio averaged 0.41 across all seasons, with minor variation. Higher *f*IPAR values were observed during the wet season and wet-dry transition. The LE/R_n ratio exhibited a significant increase during these seasons, while the dry and dry-wet transition seasons had the lowest ratios. The dry season had the highest H/R_n ratio (0.78), surpassing the wet season and wet-dry and dry-wet transitions. The G/R_n ratio was relatively small, with the dry season being the largest (4%).

3.5. Yield and efficiency responses in the use of biophysical resources

We found higher values of dry biomass during wet seasons (i.e., wet and wet-dry transition) reaching 356–361 g m^{-2} (Table S4). The cactus clearly increased its CAI during the wet-dry transition season, with an average growth of 1.14 m^2 m^{-2} and average values reaching 0.88 to 1.37 m^2 m^{-2}. Although the cactus maintained a high CAI during the dry season, it was 13.31% lower in relation to the wet-dry transition. The NAR was highest during the dry-wet transition, and 2019 showing the most significant net photosynthesis and resulting in higher RGR. In contrast, the SCA was highest during the wet-dry transition (0.001 m^2 g^{-1}) and dry season (0.001 m^2 g^{-1}), while the dry-wet transition had the lowest SCA (0.0003 m^2 g^{-1}). For the first cycle, the cactus was more productive and slightly similar in terms of cladode and morphophysiological characteristics.

The cactus showed higher nutrient and C stocks during the wet season and wet-dry transition, with the dry-wet transition season showing the third-best performance in terms of stocks (Table S4). We observed a lower efficiency in nutrient, carbon, water, and radiation use during periods with more wet conditions. Conversely, the dry and wet seasons showed higher and lower NUE and WUE, respectively. WUE was significantly higher during drier seasons, with values of 14.77 g m^{-2} mm^{-1} for the dry season and 4.56 g m^{-2} mm^{-1} for the dry-wet transition season. This contrasted with the wet season. Furthermore, we found that WUE is primarily driven by GPP. Remarkably, the wet season exhibited an RUE that was 81.48% higher than the dry season. We also found that cactus plants with high dry biomass and nitrogen and C stocks maximize their RUE.

3.6. Principal component analysis

Fig. 7 shows the PCA of the measured environment and cactus variables, providing insights into their interactions in a multivariate space. The biplots focus on the first two components (i.e., PC1 and PC2), which explain 71.57% of the variance, with 38.78% explained by PC1 and 32.79% by PC2 (Fig. 7a). The season score plot reveals a clear separation between dry seasons (left side) and wet seasons (right side). The loading plots show the relationships between variables, with loadings ranging from −0.70 to 0.71 across PCs (Fig. 7b–c).

Fig. 7b illustrates the variables that represent the nutrient-use efficiency (e.g., N, P, K, Ca, and Mg), WUE, and CUE indicate that low loadings are found in PC1 (0.23), and high loadings are found in PC2 (0.69), with a high correlation with the dry season (Fig. 7c). Dry biomass, CAI, NAR, nutrient stocks, and RUE were the main contributors to PC1 (positive and negative loadings greater than 0.5). In contrast, NEE, R_{eco}, H, G, R_g, PAR, fIPAR, WUE, and nutrient and carbon use efficiency mainly contributed to the PC2 (positive and negative charge value ≥ 0.5). When presenting highly correlated components, the environmental and plant variables pointed approximately in the same direction. Furthermore, we observed that during the dry season, there was greater expressiveness of the variables G and H (loadings: −0.7 and −0.66, respectively), with both inserted in PC2. During the dry-wet transition season, the highest negative loadings were grouped between the variables R_n (−0.39), R_g (−0.56), and PAR (−0.56) for PC2, and positively in PC1 at variables RGR, NAR, and RUE with loadings of 0.49, 0.51 and 0.7, respectively (Fig. 7b–c). In the wet and wet-dry transition seasons, we observed greater correlations between plant nutrient and C stocks, biomass, soil moisture, *LE*, APAR, R_{eco}, NEE, fIPAR, SCA and CAI. The higher the soil moisture, the higher the *LE*, APAR and R_{eco} during the wet season. Clearly, when the cactus had a high WUE (−0.69) in the dry season (entered in PC2), the R_{eco} was lower, and consequently the NEE increased. The wet-dry transition season exhibited higher values of CAI and SCA, while NAR and RGR showed a decrease. This is due to the

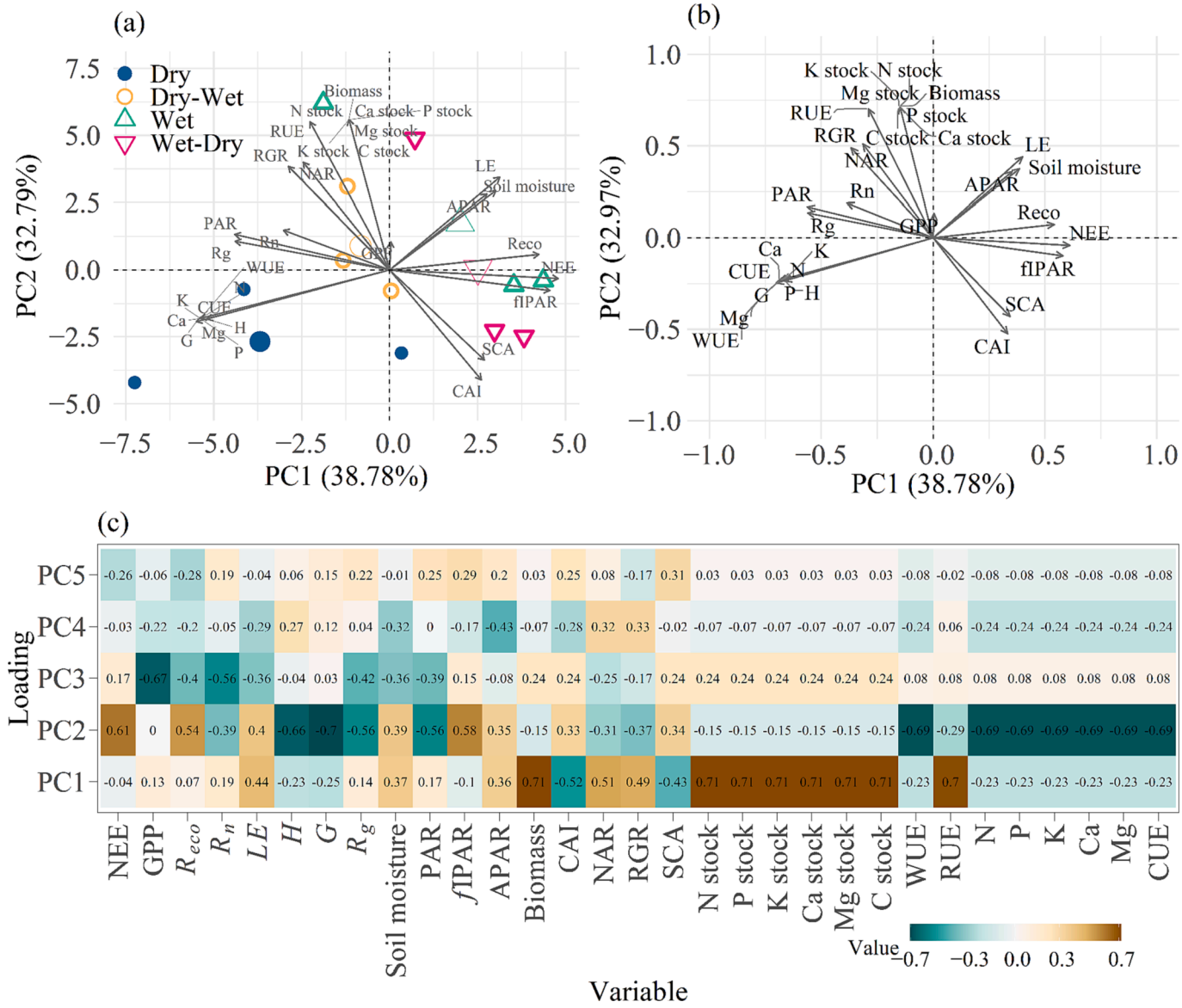

Fig. 7. Principal component analysis (PCA) shows the relationship between environmental and cactus plant variables. The panels show (a) season score variation along the first (PC1) and second (PC2) principal components, (b) variable loadings on the first two axes, and (c) component matrix with loading factors for each variable in the first five PCs with an eigenvalue greater than 1.0. For full variable names, see the Material and Methods section. The variables N, P, K, Ca and Mg mentioned represent the efficiency in the use of these nutrients. The symbols denote the four seasons (dry season, dry-wet transition, wet season and wet-dry transition) evaluated.

opposite relationships between CAI and SCA with NAR and RGR, resulting in proportional positive and negative loadings on PCs.

4. Discussion

4.1. Energy balance closure and overview of site environmental conditions

Energy balance closure in the eddy covariance system is evaluated through linear regression (Baldocchi et al., 2000; Wilson et al., 2002). A ratio of 1 between turbulent fluxes and available energy indicates a perfect closure. However, several studies report a classic lack of EBC on different vegetated surfaces when using the eddy covariance system (Campos et al., 2019; Eshonkulov et al., 2019; Flanagan and Flanagan, 2018). This study found that cactus vegetation under semi-arid conditions displayed an EBC of 0.71 (Fig. S1). A 29% imbalance in the vegetated surface may be a high value; however, it is not inconsistent (Grachev et al., 2020) and may still be satisfactory (Wilson et al., 2002). Our results are in line with the findings of Campos et al. (2019) in Caatinga (0.7), in the Brazilian semi-arid region, and lower than those reported by Owen et al. (2016) in *Agave* and *Opuntia* cultivation, in Jalisco (Mexico), with an average closure of 0.9. For example, San-José et al. (2007) reported a 0.9 energy imbalance for pineapple cultivation in Santa Barbara, Venezuela. Factors such as flat terrain, uniform growth, and absence of advection helped balance the energy.

This study's uncertainty may arise from the non-homogeneous turbulence and nighttime fluxes, which pose challenges in footprint calculations. In the case of *O. stricta* cultivation, being a CAM plant, the variation in stomatal closure and opening (day/night) may contribute to some uncertainties in the EBC. This is because nighttime (fully open stomata in cactus) and daytime (partially closed stomata in cactus) influence the latent and sensible heat fluxes, which can introduce measurement errors. Furthermore, at nighttime scale for CO_2 flux, the eddy covariance method may suffer violations under calm and stable conditions. This occurs when there is undetected CO_2 escape via non-vertical pathways (e.g., advection, drainage flows) and can lead to underestimation of nighttime respiration and overestimation of NEE (Baldocchi, 2003; Wohlfahrt et al., 2005). Although we used an open-path eddy covariance system, which minimizes high-frequency signal losses and spectral attenuation in low humidity conditions (Polonik et al., 2019), these measurement errors cannot be disregarded.

In some cases, incorporating variables such as the energy stored in the canopy and energy from photosynthesis favors the improvement of the EBC (Eshonkulov et al., 2019; Kutikoff et al., 2019). This adjustment can benefit the accuracy of the method, increasing the slope of the line and leaving the intercept close to zero (Campos et al., 2019; Kutikoff et al., 2019) when it is not forced to such a value. Seasonal variations, including fluctuations in rainfall events, could have led to an EBC imbalance (Chatterjee et al., 2021). Furthermore, the architecture of the cactus canopy, shaped by cladode positioning and biannual harvesting, might have influenced shifts in turbulent energy exchange.

Our results indicate high air temperature, high VPD, and low *RH* over the years (Fig. S2). This evidence is common in semi-arid climates with challenging environmental factors (Flanagan and Flanagan, 2018). While these conditions may hinder some species, cacti develop in harsh, high-temperature environments (Nobel and De La Barrera, 2003; Ojeda-Pérez et al., 2017; Zutta et al., 2011). In rainy months, reduced wind speed and VPD from water influx cool the environment, boosting soil moisture. Decreased wind speed may cause instability of turbulent fluxes, and thus, this could be a hypothesis for lower EBC (Flanagan and Flanagan, 2018; Teng et al., 2021). Plants can help cool the environment through transpiration and the soil through evaporation when there is high soil moisture and favorable air temperature. Furthermore, Pimienta-Barrios et al. (2000) observed that lowering air temperatures (less than 29 °C) and increasing soil moisture enhance CO_2 uptake in *O. ficus-indica* cactus. On the other hand, excessively low temperatures inhibit photosynthesis in *O. stricta* (Barker et al., 1998; Ojeda-Pérez et al., 2017).

Increased R_g input raised PAR levels, and decreased R_g led to lower PAR (Fig. S2, Fig. 2). Canopy-intercepted PAR helps to understand the photosynthetic processes of plants, and are influenced by weather and species phenology (de Cortázar and Nobel, 1986; Hartzell et al., 2021; Ma et al., 2021). de Cortázar and Nobel (1986) reported that PAR limitations can significantly compromise the performance of *O. ficus-indica*. This is because cloudiness decreases the intensity of PAR and causes a reduction in the photosynthetic efficiency of *Opuntia* (Geller and Nobel, 1987; Pimienta-Barrios et al., 2000). In addition, several species of *Opuntia* cacti may undergo changes in morphology due to the anisotropic characteristics of PAR (Drezner, 2020; Geller and Nobel, 1987). High R_g and PAR periods coincided with significant rainfall, enhancing cactus photosynthesis and light absorption. Despite water constraints, cacti sustain turgid cells due to cladode compensation during extended water scarcity (Pimienta-Barrios et al., 2000; Scalisi et al., 2016).

4.2. Changes in the balance of carbon, energy, and radiation

Due to the lower PAR magnitude during the wet-dry transition season, C uptake by plants was lower, limiting CO_2 sequestration (Nobel and Bobich, 2002). These results lead us to believe that PAR is an important modulating indicator of C uptake by cacti. Guevara-Escobar et al. (2021) also observed positive NEE results at night and more negative values during the day despite the ecosystem being composed of cacti (e.g., *O. tomentosa*, *O. robusta*, *O. hyptiacantha*, *C. imbricata*). In the present study, this may have occurred due to the presence of C3 photosynthetic species in the area (e.g., *Sida* spp.), which did not cause expressive positive NEE results during the day, as observed in crops without the interference of C3 weeds, for example, *A. tequilana* (Owen et al., 2016) and *Ananas comosus* (San-José et al., 2007). When the agroecosystem is composed of CAM, C4, and C3 photosynthesis species, there may be variations in CO_2 flux behavior, leading to limitations in identifying the CAM phases. In addition, cacti of the genus *Opuntia* may exhibit facultative C3-CAM photosynthesis, altering CO_2 flux and ET due to wet and dry seasons and cladodes development (Winter et al., 2011).

The C loss might be associated with root growth, maintenance, and soil organism respiration (Bilderback et al., 2021; De León-González et al., 2018; Nobel and Bobich, 2002). We found significant R_{eco} during the wet season (Fig. 2), which supports that rainfall stimulates the rate of heterotrophic respiration and can often equal or exceed photosynthesis daily or even seasonally (Del Grosso et al., 2018; Flores-Rentería et al., 2023). The cactus has small caliber roots—called "rain roots" that are fast growing and specialized in water absorption (Camelo et al., 2021; Hassan et al., 2019); we believe that they may have caused greater R_{eco} during the period with higher soil moisture. Snyman (2006) reported that cactus rain roots are short-lived in plants, and their decomposition contributes to microbial activity and increased soil respiration. Dubeux Junior et al. (2013) found that at a cactus plant produces 136 g of root biomass, which contributes to the heterotrophic respiration fraction and increases R_{eco}. Clearly, on days without rainfall, seasonal daytime C uptake exceeds respiration (Del Grosso et al., 2018; Flores-Rentería et al., 2023), and even with low rainfall events (~2 mm), microbial respiration in a semi-arid environment responds quickly (Huxman et al., 2004). While GPP might decrease in the dry season (Flores-Rentería et al., 2023), our study indicates that R_{eco} was more sensitive than GPP during the same period (Fig. 2, Fig. 4). The cactus's significant C sink behavior results from its perennial nature, CAM pathway, and humidity presence. This maximizes C absorption regardless of dry or wet seasons.

Solar radiation strongly stimulates photosynthesis, driving C and water exchange in ecosystems (Flanagan and Flanagan, 2018; Nobel, 1980). Conversely, insufficient water and sunlight availability can impair photosynthetic efficiency and induce photochemical damage (Han et al., 2020; Jardim et al., 2021a). According to Gao et al. (2022), the short upward radiation is mainly controlled by the short downward radiation and is influenced by ground cover. Here, we found that lower

availability of R_g and R_n influenced the C balance and decreased G, SR_u, LR_u and LR_d. In the rainy period, LE increases rapidly due to the availability of water and energy, which increases ET and water vapor exchange (Ma et al., 2022b; Zhang et al., 2022a). Although high LE values can be reached in rainy periods, the cactus still uses a substantial part of the R_n for H (Unland et al., 1996).

In the energy balance, the variables most responsive to rainfall, such as LE and G, showed greater discrepancies (Table S2). Despite notable cumulative rainfall differences, the average H difference (0.8 MJ m^{-2} day^{-1}) between the two cropping cycles (Table S2) could be linked to heightened R_n utilization for H (Unland et al., 1996). In terms of the temporal C balance, greater accumulation occurred in the cactus's initial cycle due to higher plant productivity. Even in the first cycle, ET was higher due to higher rainfall (2,075 mm) and higher GPP (3.3 g C m^{-2} day^{-1}). Although biological and abiotic factors may influence plant performance (Jardim et al., 2021a; Roeber et al., 2021), our findings clarify that the *Opuntia* cactus had a high C sink capacity throughout the experimental period. This clearly agrees with the capacity for WUE and C that CAM plants possess (Ma et al., 2022a; Pikart et al., 2018).

4.3. Flux partitioning and efficiency in the use of biophysical resources in cactus cultivation

Lower SR_u/R_g ratio responses in wet-dry transition could relate to higher CAI and SCA (Table S4) since the short upward radiation is influenced by the land cover (Gao et al., 2022) due to greater absorption of radiation by the canopy (Braghiere et al., 2020). No phenological shifts were noted in our cactus plants, with only the vegetative phase nor cladode senescence, which justifies the high similarity of the PAR/R_g ratio results (Baldocchi et al., 1984). In addition, PAR/R_g measurements were always performed at the same depth of the canopy (i.e., at the top of the canopy) since, as one approaches the ground, the PAR/R_g ratio may decrease (Baldocchi et al., 1984). Due to the plants being more developed during the wet season and wet-dry transition, as a result of the higher CAI and SCA, this development was crucial for better fIPAR responses.

Plants can lower the LE/R_n ratio under high environmental deficits to minimize water loss (Yue et al., 2019). This reduction in LE results in increased H, converting 78% of R_n into H during dry seasons. According to Campos et al. (2019) and Costa et al. (2022), in the Caatinga in the Brazilian semi-arid region, approximately 70% of R_n was converted into H, and less than 5% was converted into LE during the dry season, and these results are consistent with our study. Similar to dry forests, environments with cacti are marked by high H in relation to LE; this was also observed by Pierini et al. (2014) in a landscape of cacti (*O. spinisior* and *O. engelmannii*) in the semi-arid region of Tucson, Arizona. Despite being influenced by the H, the G/R_n ratio was equal to or less than 4%, and this ratio may change due to rainfall events and radiation incidence in cactus cultivation (Consoli et al., 2013; Flanagan and Flanagan, 2018). Flanagan and Flanagan (2018) found a mean of 2.0 MJ m^{-2} day^{-1} for G, explaining the low flux values of this variable.

Despite the expressive adaptability of *Opuntia* cactus, it has a slow relative growth rate (Luo and Nobel, 1993; Martínez-Berdeja and Valverde, 2008). Plant growth and C assimilation rates gain importance in lower humidity periods, reflecting their adaptation to reduced rainfall conditions, leading to milder responses in times of high rainfall (Jardim et al., 2023). Regarding stored nutrients and C in the cladodes, cacti have a significant accumulation of Ca^{2+}, K^+, and Mg^{2+}, being important forage foods (Garcia et al., 2021; Mayer and Cushman, 2019). K^+, for example, regulates cell osmotic potential, reducing water loss and thus increasing WUE and photochemistry (Mostofa et al., 2022). This supports our satisfactory WUE and RUE results, with the RUE being more sensitive to conditions with lower water availability. In addition, cacti can store C very similar to forest ecosystems (De León-González et al., 2018), which maximizes their exploitation potential in areas with low resource availability.

4.4. Relations between variables and environment

Clearly, the factor loadings in the PCA revealed the most important variables and their grouping in relation to environmental water availability (Mounir et al., 2020). Juhász et al. (2020) and Mounir et al. (2020) reported dispersions between seasons and the analyzed plant variables. There is a correlation between the WUE, NUE and CUE during the dry season due to the CAM pathway the plants have. Alongside elevated WUE and CUE values, these nutrients enhance cellular osmotic effects, facilitating efficient resource utilization and optimal C utilization (Ma et al., 2022a; Nobel and Bobich, 2002). The cladode and plant biomass variables were included in PC1, in agreement with the findings of Jardim et al. (2020) and Jardim et al. (2021a), using cactus species of the genus *Opuntia* and *Nopalea*. A high CAI value in cactus plants is an important indicator of high biomass yield (Dubeux Jr. et al., 2006; Jardim et al., 2021a; Jardim et al., 2020). In the wet seasons, the R_{eco} and NEE point in the same direction and with parallel vectors (Fig. 7); this shows that in the wet period, there was greater R_{eco} (positive) and higher NEE (more negative). In this way, the cultivation of *Opuntia* cactus proved to be an important atmospheric CO_2 sink, a behavior that has also been observed by Mendes et al. (2020) in Caatinga. Bilderback et al. (2021) also reported higher C losses in an environment with cacti (e.g., *O. chlorotica* and *C. acanthocarpa*) in the rainy season in the Sonoran Desert. In addition, research shows that humidity and radiation conditions can change the behavior of the energy balance and C flux in a cactus ecosystem (Camelo et al., 2021; Flanagan and Flanagan, 2018; Guevara-Escobar et al., 2021; Jardim et al., 2022).

5. Conclusions

We analyzed eddy flux covariance data over three years (2019–2021) in a cactus crop, observing the behavior of carbon, energy, and radiation balance. This work shows that in an agroecosystem cultivated with the cactus *Opuntia stricta*, the energy balance closure using data from the eddy covariance system reached satisfactory results (71%). We found that the cactus is a potential C sink throughout the year, with net ecosystem CO_2 exchange cumulative in three years of −1,130 g C m^{-2} (−377 g C m^{-2} $year^{-1}$); thus, it can be an important alternative for revitalizing degraded areas of the semi-arid region. Regardless of the season and adverse weather conditions, the cactus persisted with net CO_2 sequestration, being an important C sink. For the period 2019–2021, cumulative gross primary production and ecosystem respiration averaged 881 g C m^{-2} $year^{-1}$ and 504 g C m^{-2} $year^{-1}$, respectively. In addition, the rainfall, despite having increased the release of CO_2 from the environment, did not transform the semi-arid ecosystem of cacti into a source of carbon. Meteorological conditions act as the main drivers of physiological adjustments and plant growth. Our analyses revealed that the LE and H had marked seasonality, with most of the net radiation energy used in the H (58% ratio), with an annual average of 5.8 MJ m^{-2} day^{-1}. We found a substantial amount of nutrients in the cactus biomass and high water use efficiency and nutrients during the dry seasons. Particularly, the findings presented here bring news in studies with CAM plants and can help in the better use of agricultural land or places where agricultural and forest species may have a low capacity to develop and obtain a better balance of terrestrial carbon.

Declaration of Competing Interest

The authors declare that they have no known competing financial interests or personal relationships that could have appeared to influence the work reported in this paper.

Data availability

Data will be made available on request.

Acknowledgments

This research was supported by Portuguese funds through FCT – Foundation for Science and Technology, I.P., under the projects UIDB/04292/2020, UIDP/04292/2020, granted to MARE, and LA/P/0069/2020, granted to the Associate Laboratory ARNET. We are also grateful to the Research Support Foundation of the State of Pernambuco (FACEPE – APQ-0300-5.03/17, APQ-0215-5.01/10, and APQ-1159-1.07/14), the National Council for Scientific and Technological Development (CNPq – 152251/2018-9), the São Paulo Research Foundation (FAPESP – 17/22269-2, 2023/05323-4), and Coordination for the Improvement of Higher Education Personnel (CAPES – Finance Code 001) for the research and study grants. We also would like to thank the anonymous reviewer and the Prof. Dr. Marco Borga, Editorial Board Member, for their insightful comments that significantly improved the quality of the manuscript.

Appendix A. Supplementary data

Supplementary data to this article can be found online at https://doi.org/10.1016/j.jhydrol.2023.130121.

References

Adamič, S., Leskovšek, R., 2021. Soybean (*Glycine max* (L.) Merr.) Growth, Yield, and Nodulation in the Early Transition Period from Conventional Tillage to Conservation and No-Tillage Systems. Agronomy 11, 2477. https://doi.org/10.3390/AGRONOMY11122477.

Anapalli, S.S., Fisher, D.K., Reddy, K.N., Krutz, J.L., Pinnamaneni, S.R., Sui, R., 2019. Quantifying water and CO_2 fluxes and water use efficiencies across irrigated C_3 and C_4 crops in a humid climate. Sci. Total Environ. 663, 338–350. https://doi.org/10.1016/J.SCITOTENV.2018.12.471.

Baldocchi, D.D., 2003. Assessing the eddy covariance technique for evaluating carbon dioxide exchange rates of ecosystems: past, present and future. Glob. Chang. Biol. 9, 479–492. https://doi.org/10.1046/J.1365-2486.2003.00629.X.

Baldocchi, D., Hutchison, B., Matt, D., McMillen, R., 1984. Seasonal variations in the radiation regime within an oak-hickory forest. Agric. For. Meteorol. 33, 177–191. https://doi.org/10.1016/0168-1923(84)90069-8.

Baldocchi, D.D., Law, B.E., Anthoni, P.M., 2000. On measuring and modeling energy fluxes above the floor of a homogeneous and heterogeneous conifer forest. Agric. For. Meteorol. 102, 187–206. https://doi.org/10.1016/S0168-1923(00)00098-8.

Barker, D.H., Logan, B.A., Adams, W.W., Demmig-Adams, B., 1998. Photochemistry and xanthophyll cycle-dependent energy dissipation in differently oriented cladodes of *Opuntia stricta* during the winter. Funct. Plant Biol. 25, 95–104. https://doi.org/10.1071/PP97106.

Bilderback, A.H., Torres, A.J., Vega, M., Ball, B.A., 2021. The structural and nutrient chemistry during early-stage decomposition and desiccation of cacti in the Sonoran Desert. J. Arid Environ. 195, 104636 https://doi.org/10.1016/J.JARIDENV.2021.104636.

Braghiere, R.K., Quaife, T., Black, E., Ryu, Y., Chen, Q., De Kauwe, M.G., Baldocchi, D., 2020. Influence of sun zenith angle on canopy clumping and the resulting impacts on photosynthesis. Agric. For. Meteorol. 291, 108065 https://doi.org/10.1016/J.AGRFORMET.2020.108065.

Camelo, D., Dubeux, J.C.B., dos Santos, M.V.F., Lira, M.A., Fracetto, G.G.M., Fracetto, F. J.C., da Cunha, M.V., de Freitas, E.V., 2021. Soil Microbial Activity and Biomass in Semiarid Agroforestry Systems Integrating Forage Cactus and Tree Legumes. Agronomy 11 (8), 1558.

Campos, S., Mendes, K.R., da Silva, L.L., Mutti, P.R., Medeiros, S.S., Amorim, L.B., dos Santos, C.A.C., Perez-Marin, A.M., Ramos, T.M., Marques, T.V., Lucio, P.S., Costa, G. B., Santos e Silva, C.M., Bezerra, B.G., 2019. Closure and partitioning of the energy balance in a preserved area of a Brazilian seasonally dry tropical forest. Agric. For. Meteorol. 271, 398–412.

Chatterjee, D., Kumar Swain, C., Chatterjee, S., Bhattacharyya, P., Tripathi, R., Lal, B., Gautam, P., Shahid, M., Kumar Dash, P., Dhal, B., Kumar Nayak, A., Chatterjee, D., Kumar Swain, C., Chatterjee, S., Bhattacharyya, P., Tripathi, R., Lal, B., Gautam, P., Shahid, M., Kumar Dash, P., Dhal, B., Kumar Nayak, A., 2021. Is the energy balance in a tropical lowland rice paddy perfectly closed? Atmósfera 34, 59–78. https://doi.org/10.20937/ATM.52734.

Coêlho, D. de L., Dubeux Jr., J.C.B., Santos, M.V.F. dos, Mello, A.C.L. de, Cunha, M.V. da, Santos, D.C. dos, Freitas, E.V. de, Santos, E.R. da S., 2023. Soil and Root System Attributes of Forage Cactus under Different Management Practices in the Brazilian Semiarid. Agronomy 13, 743. https://doi.org/10.3390/AGRONOMY13030743.

Consoli, S., Inglese, G., Inglese, P., 2013. Determination of Evapotranspiration and Annual Biomass Productivity of a Cactus Pear [*Opuntia ficus-indica* L. (Mill.)] Orchard in a Semiarid Environment. J. Irrig. Drain. Eng. 139, 680–690. https://doi.org/10.1061/(ASCE)IR.1943-4774.0000589.

Costa, G.B., Mendes, K.R., Viana, L.B., Almeida, G.V., Mutti, P.R., Silva, C.M.S., Bezerra, B.G., Marques, T.V., Ferreira, R.R., Oliveira, C.P., Gonçalves, W.A., Oliveira, P.E., Campos, S., Andrade, M.U.G., Antonino, A.C.D., Menezes, R.S.C., 2022. Seasonal Ecosystem Productivity in a Seasonally Dry Tropical Forest (Caatinga) Using Flux Tower Measurements and Remote Sensing Data. Remote Sens. 14, 3955. https://doi.org/10.3390/RS14163955.

Cunliffe, A.M., Boschetti, F., Clement, R., Sitch, S., Anderson, K., Duman, T., Zhu, S., Schlumpf, M., Litvak, M.E., Brazier, R.E., Hill, T.C., 2022. Strong Correspondence in Evapotranspiration and Carbon Dioxide Fluxes Between Different Eddy Covariance Systems Enables Quantification of Landscape Heterogeneity in Dryland Fluxes. J. Geophys. Res. Biogeosciences 127, e2021JG006240. https://doi.org/10.1029/2021JG006240.

Silva, T.G.F. da, Medeiros, R.S. de, Arraes, F.D.D., Ramos, C.M.C., Araújo Júnior, G. do N., Jardim, A.M. da R.F., Alves, C.P., Campos, F.S., da Silva, M.V., de Morais, J.E.F., de Souza, C.A.A., Siqueira e Silva, S.M., dos Santos, D.C., de Carvalho, A.A., Souza, L. S.B. de, 2023. Cactus–sorghum intercropping combined with management interventions of planting density, row orientation and nitrogen fertilisation can optimise water use in dry regions. Sci. Total Environ. 895, 165102. https://doi.org/10.1016/J.SCITOTENV.2023.165102.

de Cortázar, V.G., Nobel, P.S., 1986. Modeling of PAR Interception and Productivity of a Prickly Pear Cactus, *Opuntia ficus-indica* L., at Various Spacings1. Agron. J. 78, 80–85. https://doi.org/10.2134/AGRONJ1986.00021962007800010018X.

De León-González, F., Fuentes-Ponce, M.H., Bautista-Cruz, A., Leyva-Pablo, T., Castillo-Juárez, H., Rodríguez-Sánchez, L.M., 2018. Cactus crop as an option to reduce soil C-CO_2 emissions in soils with declining fertility. Agron. Sustain. Dev. 38, 1–10. https://doi.org/10.1007/S13593-017-0481-3/TABLES/1.

Del Grosso, S.J., Parton, W.J., Derner, J.D., Chen, M., Tucker, C.J., 2018. Simple models to predict grassland ecosystem C exchange and actual evapotranspiration using NDVI and environmental variables. Agric. For. Meteorol. 249, 1–10. https://doi.org/10.1016/J.AGRFORMET.2017.11.007.

Dhungel, R., Aiken, R., Evett, S.R., Colaizzi, P.D., Marek, G., Moorhead, J.E., Baumhardt, R.L., Brauer, D., Kutikoff, S., Lin, X., 2021. Energy Imbalance and Evapotranspiration Hysteresis Under an Advective Environment: Evidence From Lysimeter, Eddy Covariance, and Energy Balance Modeling. Geophys. Res. Lett. 48, e2020GL091203. https://doi.org/10.1029/2020GL091203.

Drezner, T.D., 2020. The importance of microenvironment: *Opuntia* plant growth, form and the response to sunlight. J. Arid Environ. 178, 104144 https://doi.org/10.1016/J.JARIDENV.2020.104144.

Du Toit, A., De Wit, M., Hugo, A., 2018. Cultivar and Harvest Month Influence the Nutrient Content of Opuntia spp. Cactus Pear Cladode Mucilage Extracts. Molecules 23, 916. https://doi.org/10.3390/MOLECULES23040916.

Dubeux Jr., J.C.B., dos Santos, M.V.F., de Andrade Lira, M., dos Santos, D.C., Farias, I., Lima, L.E., Ferreira, R.L.C., 2006. Productivity of *Opuntia ficus-indica* (L.) Miller under different N and P fertilization and plant population in north-east Brazil. J. Arid Environ. 67 (3), 357–372.

Dubeux Jr., J.C.B., Santos, M.V.F. dos, Cunha, M.V. da, Santos, D.C. dos, Souza, R.T. de A., Mello, A.C.L. de, Souza, T.C. de, 2021. Cactus (*Opuntia* and *Nopalea*) nutritive value: A review. Anim. Feed Sci. Technol. 275, 114890. https://doi.org/10.1016/J.ANIFEEDSCI.2021.114890.

Dubeux Junior, J.C.B., Silva, N.G.M., Santos, M.V.F., Cunha, M.V., Santos, D.C., Lira, M. A., Mello, A.C.L., Pinto, M.S.C., 2013. Organic fertilization and plant population affect shoot and root biomass of forage cactus pear (*Opuntia ficus-indica* Mill.). Acta Hortic. 995, 221–224. https://doi.org/10.17660/ACTAHORTIC.2013.995.25.

Eshonkulov, R., Poyda, A., Ingwersen, J., Pulatov, A., Streck, T., 2019. Improving the energy balance closure over a winter wheat field by accounting for minor storage terms. Agric. For. Meteorol. 264, 283–296. https://doi.org/10.1016/J.AGRFORMET.2018.10.012.

Flanagan, L.B., Flanagan, J.E.M., 2018. Seasonal controls on ecosystem-scale CO_2 and energy exchange in a Sonoran Desert characterized by the saguaro cactus (*Carnegiea gigantea*). Oecologia 187, 977–994. https://doi.org/10.1007/S00442-018-4187-2/FIGURES/10.

Flores-Rentería, D., Delgado-Balbuena, J., Campuzano, E.F., Curiel Yuste, J., 2023. Seasonal controlling factors of CO_2 exchange in a semiarid shrubland in the Chihuahuan Desert. Mexico. Sci. Total Environ. 858, 159918 https://doi.org/10.1016/J.SCITOTENV.2022.159918.

Gao, X., Du, Z., Yang, Q., Zhang, J., Li, Y., Wang, X., Gu, F., Hao, W., Yang, Z., Liu, D., Chu, J., 2022. Energy partitioning and evapotranspiration in a black locust plantation on the Yellow River Delta. China. J. For. Res. 33, 1219–1232. https://doi.org/10.1007/S11676-021-01376-Y/FIGURES/7.

Garcia, C.V., Mello, A.C.L., Cunha, M.V.d., Silva, M.d.C., Santos, D.C.D., Santos, M.V.F., Dubeux, J.C.B., Homem, B.G.C., 2021. Agronomic characteristics and nutritional value of cactus pear progenies. Agron. J. 113 (6), 4721–4735.

Geller, G.N., Nobel, P.S., 1987. Comparative Cactus Architecture and PAR Interception. Am. J. Bot. 74, 998–1005. https://doi.org/10.1002/J.1537-2197.1987.TB08709.X.

Grachev, A.A., Fairall, C.W., Blomquist, B.W., Fernando, H.J.S., Leo, L.S., Otárola-Bustos, S.F., Wilczak, J.M., McCaffrey, K.L., 2020. On the surface energy balance closure at different temporal scales. Agric. For. Meteorol. 281, 107823 https://doi.org/10.1016/J.AGRFORMET.2019.107823.

Guevara-Escobar, A., González-Sosa, E., Cervantes-Jimenez, M., Suzán-Azpiri, H., Queijeiro-Bolanos, M.E., Carrillo-Ángeles, I., Cambron-Sandoval, V.H., 2021. Machine learning estimates of eddy covariance carbon flux in a scrub in the Mexican highland. Biogeosciences 18, 367–392. https://doi.org/10.5194/BG-18-367-2021.

Han, J., Guo, C., Ye, S., Zhang, L., Li, S., Wang, H., Yu, G., 2020. Effects of diffuse photosynthetically active radiation on gross primary productivity in a subtropical coniferous plantation vary in different timescales. Ecol. Indic. 115, 106403 https://doi.org/10.1016/J.ECOLIND.2020.106403.

Hartzell, S., Bartlett, M.S., Inglese, P., Consoli, S., Yin, J., Porporato, A., 2021. Modelling nonlinear dynamics of Crassulacean acid metabolism productivity and water use for

global predictions. Plant. Cell Environ. 44, 34–48. https://doi.org/10.1111/PCE.13918.
Hassan, S., Inglese, P., Gristina, L., Liguori, G., Novara, A., Louhaichi, M., Sortino, G., 2019. Root growth and soil carbon turnover in *Opuntia ficus-indica* as affected by soil volume availability. Eur. J. Agron. 105, 104–110. https://doi.org/10.1016/J.EJA.2019.02.012.
Huxman, T.E., Snyder, K.A., Tissue, D., Leffler, A.J., Ogle, K., Pockman, W.T., Sandquist, D.R., Potts, D.L., Schwinning, S., 2004. Precipitation pulses and carbon fluxes in semiarid and arid ecosystems. Oecologia 141, 254–268. https://doi.org/10.1007/S00442-004-1682-4/FIGURES/6.
Jardim, A.M.d.R.F., Santos, H.R.B., Alves, H.K.M.N., Ferreira-Silva, S.L., Souza, L.S.B.d., Araújo Júnior, G.d.N., Souza, M.d.S., Araújo, G.G.L.d., Souza, C.A.A.d., Silva, T.G.F.d., 2021a. Genotypic differences relative photochemical activity, inorganic and organic solutes and yield performance in clones of the forage cactus under semi-arid environment. Plant Physiol. Biochem. 162, 421–430.
Jardim, A.M.R.F., Silva, T.G.F., Souza, L.S.B., Souza, M.S., Morais, J.E.F., Araújo Júnior, G.N., 2020. Multivariate analysis in the morpho-yield evaluation of forage cactus intercropped with sorghum. Rev. Bras. Eng. Agrícola e Ambient. 24, 756–761. https://doi.org/10.1590/1807-1929/AGRIAMBI.V24N11P756-761.
Jardim, A.M.R.F., de Souza, L.S.B., Alves, C.P., Ferreira Nunes de Araújo, J., de Souza, C.A.A., Pinheiro, A.G., de Araújo, G.G.L., Campos, F.S., Tabosa, J.N., Silva, T.G.F.d., 2023. Intercropping forage cactus with sorghum affects the morphophysiology and phenology of forage cactus. African J. Range Forage Sci. 40 (2), 129–140.
Jardim, A.M.R.F., Morais, J.E.F., Souza, L.S.B., Silva, T.G.F., 2022. Understanding interactive processes: a review of CO_2 flux, evapotranspiration, and energy partitioning under stressful conditions in dry forest and agricultural environments. Environ. Monit. Assess. 194, 1–22. https://doi.org/10.1007/S10661-022-10339-7.
Jardim, A.M.d.R.F., Silva, T.G.F.d., Souza, L.S.B.d., Araújo Júnior, G.d.N., Alves, H.K.M.N., Souza, M.d.S., Araújo, G.G.L.d., Moura, M.S.B.d., 2021b. Intercropping forage cactus and sorghum in a semi-arid environment improves biological efficiency and competitive ability through interspecific complementarity. J. Arid Environ. 188 https://doi.org/10.1016/J.JARIDENV.2021.104464.
Juhász, C., Gálya, B., Kovács, E., Nagy, A., Tamás, J., Huzsvai, L., 2020. Seasonal predictability of weather and crop yield in regions of Central European continental climate. Comput. Electron. Agric. 173, 105400 https://doi.org/10.1016/J.COMPAG.2020.105400.
Kaiser, H.F., 1960. The application of electronic computers to factor analysis. Educ. Psychol. Meas. 20, 141–151. https://doi.org/10.1177/001316446002000116.
Khapte, P.S., Kumar, P., Wakchaure, G.C., Jangid, K.K., Colla, G., Cardarelli, M., Rane, J., 2022. Application of Phenomics to Elucidate the Influence of Rootstocks on Drought Response of Tomato. Agronomy 12, 1529. https://doi.org/10.3390/AGRONOMY12071529.
Kumar, S., Louhaichi, M., Dana Ram, P., Tirumala, K.K., Ahmad, S., Rai, A.K., Sarker, A., Hassan, S., Liguori, G., Probir Kumar, G., Govindasamy, P., Prasad, M., Mahawer, S. K., Appaswamygowda, B.H., 2021. Cactus Pear (*Opuntia ficus-indica*) Productivity, Proximal Composition and Soil Parameters as Affected by Planting Time and Agronomic Management in a Semi-Arid Region of India. Agronomy 11, 1647. https://doi.org/10.3390/AGRONOMY11081647.
Kutikoff, S., Lin, X., Evett, S., Gowda, P., Moorhead, J., Marek, G., Colaizzi, P., Aiken, R., Brauer, D., 2019. Heat storage and its effect on the surface energy balance closure under advective conditions. Agric. For. Meteorol. 265, 56–69. https://doi.org/10.1016/J.AGRFORMET.2018.10.018.
Lamichhane, S., Eğilmez, G., Gedik, R., Bhutta, M.K.S., Erenay, B., 2021. Benchmarking OECD countries' sustainable development performance: A goal-specific principal component analysis approach. J. Clean. Prod. 287, 125040 https://doi.org/10.1016/J.JCLEPRO.2020.125040.
Leite-Filho, A.T., de Sousa Pontes, V.Y., Costa, M.H., 2019. Effects of Deforestation on the Onset of the Rainy Season and the Duration of Dry Spells in Southern Amazonia. J. Geophys. Res. Atmos. 124, 5268–5281. https://doi.org/10.1029/2018JD029537.
Loupassaki, M.H., Chartzoulakis, K.S., Digalaki, N.B., Androulakis, I.I., 2007. Effects of salt stress on concentration of nitrogen, phosphorus, potassium, calcium, magnesium, and sodium in leaves, shoots, and roots of six olive cultivars. J. Plant Nutr. 25, 2457–2482. https://doi.org/10.1081/PLN-120014707.
Luo, Y., Nobel, P.S., 1993. Growth characteristics of newly initiated cladodes of Opuntia ficus-indica as affected by shading, drought and elevated CO2. Physiol. Plant. 87, 467–474. https://doi.org/10.1111/J.1399-3054.1993.TB02495.X.
Ma, H., Li, L., Liu, S., Shi, W., Wang, C., Zhao, Q., Cui, N., Wang, Y., 2022a. Physiological response, phytohormone signaling, biomass production and water use efficiency of the CAM plant Ananas comosus under different water and nitrogen regimes. Agric. Water Manag. 266, 107563 https://doi.org/10.1016/J.AGWAT.2022.107563.
Ma, J., Wen, X., Li, M., Luo, S., Zhu, X., Yang, X., Chen, M., 2022b. Analysis of Surface Energy Changes over Different Underlying Surfaces Based on MODIS Land-Use Data and Green Vegetation Fraction over the Tibetan Plateau. Remote Sens. 14, 2751. https://doi.org/10.3390/RS14122751.
Ma, L., Zheng, G., Ying, Q., Hancock, S., Ju, W., Yu, D., 2021. Characterizing the three-dimensional spatiotemporal variation of forest photosynthetically active radiation using terrestrial laser scanning data. Agric. For. Meteorol. 301–302, 108346 https://doi.org/10.1016/J.AGRFORMET.2021.108346.
Martínez-Berdeja, A., Valverde, T., 2008. Growth response of three globose cacti to radiation and soil moisture: An experimental test of the mechanism behind the nurse effect. J. Arid Environ. 72, 1766–1774. https://doi.org/10.1016/J.JARIDENV.2008.04.010.
Mayer, J.A., Cushman, J.C., 2019. Nutritional and mineral content of prickly pear cactus: A highly water-use efficient forage, fodder and food species. J. Agron. Crop Sci. 205, 625–634. https://doi.org/10.1111/JAC.12353.
McGloin, R., Šigut, L., Havránková, K., Dušek, J., Pavelka, M., Sedlák, P., 2018. Energy balance closure at a variety of ecosystems in Central Europe with contrasting topographies. Agric. For. Meteorol. 248, 418–431. https://doi.org/10.1016/J.AGRFORMET.2017.10.003.
Mendes, K.R., Campos, S., da Silva, L.L., Mutti, P.R., Ferreira, R.R., Medeiros, S.S., Perez-Marin, A.M., Marques, T.V., Ramos, T.M., de Lima Vieira, M.M., Oliveira, C.P., Gonçalves, W.A., Costa, G.B., Antonino, A.C.D., Menezes, R.S.C., Bezerra, B.G., Santos e Silva, C.M., 2020. Seasonal variation in net ecosystem CO_2 exchange of a Brazilian seasonally dry tropical forest. Sci. Rep. 10 (1) https://doi.org/10.1038/s41598-020-66415-w.
Moore, C.J., 1986. Frequency response corrections for eddy correlation systems. Boundary-Layer Meteorol. 37, 17–35. https://doi.org/10.1007/BF00122754.
Mostofa, M.G., Rahman, M.M., Ghosh, T.K., Kabir, A.H., Abdelrahman, M., Rahman Khan, M.A., Mochida, K., Tran, L.S.P., 2022. Potassium in plant physiological adaptation to abiotic stresses. Plant Physiol. Biochem. 186, 279–289. https://doi.org/10.1016/J.PLAPHY.2022.07.011.
Mounir, B., Younes, E.G., Asmaa, M., Abdeljalil, Z., Abdellah, A., 2020. Physico-chemical changes in cladodes of *Opuntia ficus-indica* as a function of the growth stage and harvesting areas. J. Plant Physiol. 251, 153196 https://doi.org/10.1016/J.JPLPH.2020.153196.
Nobel, P.S., 1980. Interception of photosynthetically active radiation by cacti of different morphology. Oecologia 45, 160–166. https://doi.org/10.1007/BF00346455.
Nobel, P.S., Bobich, E.G., 2002. Initial Net CO_2 Uptake Responses and Root Growth for a CAM Community Placed in a Closed Environment. Ann. Bot. 90, 593–598. https://doi.org/10.1093/AOB/MCF229.
Nobel, P.S., De La Barrera, E., 2003. Tolerances and acclimation to low and high temperatures for cladodes, fruits and roots of a widely cultivated cactus. *Opuntia ficus-indica*. New Phytol. 157, 271–279. https://doi.org/10.1046/J.1469-8137.2003.00675.X.
Ojeda-Pérez, Z.Z., Jiménez-Bremont, J.F., Delgado-Sánchez, P., Blazquez, M.A., 2017. Continuous high and low temperature induced a decrease of photosynthetic activity and changes in the diurnal fluctuations of organic acids in *Opuntia streptacantha*. PLoS One 12 (10), e0186540.
Owen, N.A., Choncubhair, Ó.N., Males, J., del Real Laborde, J.I., Rubio-Cortés, R., Griffiths, H., Lanigan, G., 2016. Eddy covariance captures four-phase crassulacean acid metabolism (CAM) gas exchange signature in *Agave*. Plant. Cell Environ. 39, 295–309. https://doi.org/10.1111/PCE.12610.
Papale, D., Reichstein, M., Aubinet, M., Canfora, E., Bernhofer, C., Kutsch, W., Longdoz, B., Rambal, S., Valentini, R., Vesala, T., Yakir, D., 2006. Towards a standardized processing of Net Ecosystem Exchange measured with eddy covariance technique: Algorithms and uncertainty estimation. Biogeosciences 3, 571–583. https://doi.org/10.5194/BG-3-571-2006.
Pierini, N.A., Vivoni, E.R., Robles-Morua, A., Scott, R.L., Nearing, M.A., 2014. Using observations and a distributed hydrologic model to explore runoff thresholds linked with mesquite encroachment in the Sonoran Desert. Water Resour. Res. 50, 8191–8215. https://doi.org/10.1002/2014WR015781.
Pikart, F.C., Marabesi, M.A., Mioto, P.T., Gonçalves, A.Z., Matiz, A., Alves, F.R.R., Mercier, H., Aidar, M.P.M., 2018. The contribution of weak CAM to the photosynthetic metabolic activities of a bromeliad species under water deficit. Plant Physiol. Biochem. 123, 297–303. https://doi.org/10.1016/J.PLAPHY.2017.12.030.
Pimienta-Barrios, E., Zañudo, J., Yepez, E., Pimienta-Barrios, E., Nobel, P.S., 2000. Seasonal variation of net CO_2 uptake for cactus pear (*Opuntia ficus-indica*) and pitayo (*Stenocereus queretaroensis*) in a semi-arid environment. J. Arid Environ. 44, 73–83. https://doi.org/10.1006/JARE.1999.0570.
Pinheiro, K.M., Silva, T.G.F.d., Carvalho, H.F.d.S., Santos, J.E.O., Morais, J.E.F.d., Zolnier, S., Santos, D.C.D., 2014. Correlações do índice de área do cladódio com características morfogênicas e produtivas da palma forrageira. Pesqui. Agropecuária Bras. 49 (12), 939–947.
Polonik, P., Chan, W.S., Billesbach, D.P., Burba, G., Li, J., Nottrott, A., Bogoev, I., Conrad, B., Biraud, S.C., 2019. Comparison of gas analyzers for eddy covariance: Effects of analyzer type and spectral corrections on fluxes. Agric. For. Meteorol. 272–273, 128–142. https://doi.org/10.1016/J.AGRFORMET.2019.02.010.
R Core Team, 2022. R: The R Project for Statistical Computing.
Rannik, Ü., Vesala, T., 1999. Autoregressive filtering versus linear detrending in estimation of fluxes by the eddy covariance method. Boundary-Layer Meteorol. 91, 259–280. https://doi.org/10.1023/A:1001840416858.
Raza, M.A., Feng, L.Y., Werf, W., Cai, G.R., Khalid, M.H.B., Iqbal, N., Hassan, M.J., Meraj, T.A., Naeem, M., Khan, I., Rehman, S.u., Ansar, M., Ahmed, M., Yang, F., Yang, W., 2019. Narrow-wide-row planting pattern increases the radiation use efficiency and seed yield of intercrop species in relay-intercropping system. Food Energy Secur. 8 (3), e170. https://doi.org/10.1002/FES3.170.
Rodda, S.R., Thumaty, K.C., Praveen, M.S.S., Jha, C.S., Dadhwal, V.K., 2021. Multi-year eddy covariance measurements of net ecosystem exchange in tropical dry deciduous forest of India. Agric. For. Meteorol. 301–302, 108351 https://doi.org/10.1016/J.AGRFORMET.2021.108351.
Rodrigues, C.R.F., Silva, E.N., Ferreira-Silva, S.L., Voigt, E.L., Viégas, R.A., Silveira, J.A. G., 2013. High K^+ supply avoids Na^+ toxicity and improves photosynthesis by allowing favorable K^+ : Na^+ ratios through the inhibition of Na^+ uptake and transport to the shoots of *Jatropha curcas* plants. J. Plant Nutr. Soil Sci. 176, 157–164. https://doi.org/10.1002/JPLN.201200230.
Roeber, V.M., Bajaj, I., Rohde, M., Schmülling, T., Cortleven, A., 2021. Light acts as a stressor and influences abiotic and biotic stress responses in plants. Plant. Cell Environ. 44, 645–664. https://doi.org/10.1111/PCE.13948.
Salack, S., Klein, C., Giannini, A., Sarr, B., Worou, O.N., Belko, N., Bliefernicht, J., Kunstman, H., 2016. Global warming induced hybrid rainy seasons in the Sahel. Environ. Res. Lett. 11, 104008 https://doi.org/10.1088/1748-9326/11/10/104008.

Salazar-Martínez, D., Holwerda, F., Holmes, T.R.H., Yépez, E.A., Hain, C.R., Alvarado-Barrientos, S., Ángeles-Pérez, G., Arredondo-Moreno, T., Delgado-Balbuena, J., Figueroa-Espinoza, B., Garatuza-Payán, J., González del Castillo, E., Rodríguez, J.C., Rojas-Robles, N.E., Uuh-Sonda, J.M., Vivoni, E.R., 2022. Evaluation of remote sensing-based evapotranspiration products at low-latitude eddy covariance sites. J. Hydrol. 610, 127786 https://doi.org/10.1016/J.JHYDROL.2022.127786.

Saliendra, N.Z., Liebig, M.A., Kronberg, S.L., 2018. Carbon use efficiency of hayed alfalfa and grass pastures in a semiarid environment. Ecosphere 9 (3), e02147.

San-José, J., Montes, R., Nikonova, N., 2007. Diurnal patterns of carbon dioxide, water vapour, and energy fluxes in pineapple [*Ananas comosus* (L.) Merr. cv. Red Spanish] field using eddy covariance. Photosynthetica 45, 370–384. https://doi.org/10.1007/S11099-007-0064-7.

Santos, F.N.S., Santos, E.M., Oliveira, J.S., Medeiros, G.R., Zanine, A.M., Araújo, G.G.L., Perazzo, A.F., Lemos, M.L.P., Pereira, D.M., Cruz, G.F.L., Paulino, R.S., Oliveira, C.J. B., 2020. Fermentation profile, microbial populations, taxonomic diversity and aerobic stability of total mixed ration silages based on Cactus and Gliricidia. J. Agric. Sci. 158, 396–405. https://doi.org/10.1017/S0021859620000805.

Scalisi, A., Morandi, B., Inglese, P., Lo Bianco, R., 2016. Cladode growth dynamics in *Opuntia ficus-indica* under drought. Environ. Exp. Bot. 122, 158–167. https://doi.org/10.1016/J.ENVEXPBOT.2015.10.003.

Schotanus, P., Nieuwstadt, F.T.M., De Bruin, H.A.R., 1983. Temperature measurement with a sonic anemometer and its application to heat and moisture fluxes. Boundary-Layer Meteorol. 26, 81–93. https://doi.org/10.1007/BF00164332.

Siddiq, Z., Hayyat, M.U., Khan, A.U., Mahmood, R., Shahzad, L., Ghaffar, R., Cao, K.F., 2021. Models to estimate the above and below ground carbon stocks from a subtropical scrub forest of Pakistan. Glob. Ecol. Conserv. 27, e01539.

Silva, M.S., Nóbrega, J.S., Santos, C.C., Costa, F.B., Abreu, D.C., Silva, W.M., Hoshide, A. K., Gomes, F.A.L., Pereira, U.S., Linné, J.A., Scalon, S.P.Q., 2023. Organic Fertilization with Biofertilizer Alters the Physical and Chemical Characteristics of Young Cladodes of *Opuntia stricta* (Haw.) Haw. Sustainability 15, 3841. https://doi.org/10.3390/SU15043841.

Silva, T.G.F., Miranda, K.R., Santos, D.C., Queiroz, M.G., Silva, M.C., Cruz Neto, J.F., Araújo, J.E.M., 2014. Área do cladódio de clones de palma forrageira: modelagem, análise e aplicabilidade. Rev. Bras. Ciências Agrárias 9, 626–632. https://doi.org/10.5039/AGRARIA.V9I4A4553.

Snyman, H.A., 2006. A greenhouse study on root dynamics of cactus pears, *Opuntia ficus-indica* and *O. robusta*. J. Arid Environ. 65, 529–542. https://doi.org/10.1016/J.JARIDENV.2005.10.004.

Teng, D., He, X., Qin, L., Lv, G., 2021. Energy Balance Closure in the Tugai Forest in Ebinur Lake Basin. Northwest China. Forests 12, 243. https://doi.org/10.3390/F12020243.

Unland, H.E., Houser, P.R., Shuttleworth, W.J., Yang, Z.L., 1996. Surface flux measurement and modeling at a semi-arid Sonoran Desert site. Agric. For. Meteorol. 82, 119–153. https://doi.org/10.1016/0168-1923(96)02330-1.

Vickers, D., Mahrt, L., 1974. Quality Control and Flux Sampling Problems for Tower and Aircraft Data. J. Atmos. Ocean. Technol. 7, 363–372. https://doi.org/10.1007/BF00240838.

Webb, E.K., Pearman, G.I., Leuning, R., 1980. Correction of flux measurements for density effects due to heat and water vapour transfer. Q. J. R. Meteorol. Soc. 106, 85–100. https://doi.org/10.1002/QJ.49710644707.

Widmoser, P., Wohlfahrt, G., 2018. Attributing the energy imbalance by concurrent lysimeter and eddy covariance evapotranspiration measurements. Agric. For. Meteorol. 263, 287–291. https://doi.org/10.1016/J.AGRFORMET.2018.09.003.

Wilczak, J.M., Oncley, S.P., Stage, S.A., 2001. Sonic Anemometer Tilt Correction Algorithms. Boundary-Layer Meteorol. 99, 127–150. https://doi.org/10.1023/A:1018966204465.

Wilson, K., Goldstein, A., Falge, E., Aubinet, M., Baldocchi, D., Berbigier, P., Bernhofer, C., Ceulemans, R., Dolman, H., Field, C., Grelle, A., Ibrom, A., Law, B.E., Kowalski, A., Meyers, T., Moncrieff, J., Monson, R., Oechel, W., Tenhunen, J., Valentini, R., Verma, S., 2002. Energy balance closure at FLUXNET sites. Agric. For. Meteorol. 113, 223–243. https://doi.org/10.1016/S0168-1923(02)00109-0.

Winter, K., Garcia, M., Holtum, J.A.M., 2011. Drought-stress-induced up-regulation of CAM in seedlings of a tropical cactus, *Opuntia elatior*, operating predominantly in the C_3 mode. J. Exp. Bot. 62, 4037–4042. https://doi.org/10.1093/JXB/ERR106.

Wohlfahrt, G., Anfang, C., Bahn, M., Haslwanter, A., Newesely, C., Schmitt, M., Drösler, M., Pfadenhauer, J., Cernusca, A., 2005. Quantifying nighttime ecosystem respiration of a meadow using eddy covariance, chambers and modelling. Agric. For. Meteorol. 128, 141–162. https://doi.org/10.1016/J.AGRFORMET.2004.11.003.

Wutzler, T., Lucas-Moffat, A., Migliavacca, M., Knauer, J., Sickel, K., Šigut, L., Menzer, O., Reichstein, M., 2018. Basic and extensible post-processing of eddy covariance flux data with REddyProc. Biogeosciences 15, 5015–5030. https://doi.org/10.5194/BG-15-5015-2018.

Yang, F., Huang, J., Zheng, X., Huo, W., Zhou, C., Wang, Y., Han, D., Gao, J., Mamtimin, A., Yang, X., Sun, Y., 2022. Evaluation of carbon sink in the Taklimakan Desert based on correction of abnormal negative CO_2 flux of IRGASON. Sci. Total Environ. 838, 155988 https://doi.org/10.1016/J.SCITOTENV.2022.155988.

Yao, Y., Li, Z., Wang, T., Chen, A., Wang, X., Du, M., Jia, G., Li, Y., Li, H., Luo, W., Ma, Y., Tang, Y., Wang, H., Wu, Z., Yan, J., Zhang, X., Zhang, Y., Zhang, Y.u., Zhou, G., Piao, S., 2018. A new estimation of China's net ecosystem productivity based on eddy covariance measurements and a model tree ensemble approach. Agric. For. Meteorol. 253–254, 84–93. https://doi.org/10.1016/J.AGRFORMET.2018.02.007.

Yue, P., Zhang, Q., Zhang, L., Li, H., Yang, Y., Zeng, J., Wang, S., 2019. Long-term variations in energy partitioning and evapotranspiration in a semiarid grassland in the Loess Plateau of China. Agric. For. Meteorol. 278, 107671 https://doi.org/10.1016/J.AGRFORMET.2019.107671.

Zeng, J., Matsunaga, T., Tan, Z.H., Saigusa, N., Shirai, T., Tang, Y., Peng, S., Fukuda, Y., 2020. Global terrestrial carbon fluxes of 1999–2019 estimated by upscaling eddy covariance data with a random forest. Sci. Data 7, 1–11. https://doi.org/10.1038/s41597-020-00653-5.

Zhang, K., Liu, D., Liu, H., Lei, H., Guo, F., Xie, S., Meng, X., Huang, Q., 2022a. Energy flux observation in a shrub ecosystem of a gully region of the Chinese Loess Plateau. Ecohydrol. Hydrobiol. 22, 323–336. https://doi.org/10.1016/J.ECOHYD.2021.10.001.

Zhang, Q., Song, Y., Wu, Z., Yan, X., Gunina, A., Kuzyakov, Y., Xiong, Z., 2020. Effects of six-year biochar amendment on soil aggregation, crop growth, and nitrogen and phosphorus use efficiencies in a rice-wheat rotation. J. Clean. Prod. 242, 118435 https://doi.org/10.1016/J.JCLEPRO.2019.118435.

Zhang, K., Wang, X., Li, Y., Zhao, J., Yang, Y., Zang, H., Zeng, Z., 2022b. Peanut residue incorporation benefits crop yield, nitrogen yield, and water use efficiency of summer peanut – winter wheat systems. F. Crop. Res. 279, 108463 https://doi.org/10.1016/J.FCR.2022.108463.

Zutta, B.R., Nobel, P.S., Aramians, A.M., Sahaghian, A., 2011. Low- and High-Temperature Tolerance and Acclimation for Chlorenchyma versus Meristem of the Cultivated Cacti *Nopalea cochenillifera*, *Opuntia robusta*, and *Selenicereus megalanthus*. J. Bot. 2011, 1–6. https://doi.org/10.1155/2011/347168.